Continuous-Time Markov Chain and Regime Switching Approximations with Applications to Options Pricing

Zhenyu Cui, J. Lars Kirkby and Duy Nguyen

Abstract In this chapter, we present recent developments in using the tools of continuous-time Markov chains for the valuation of European and path-dependent financial derivatives. We also survey results on a newly proposed regime switching approximation to stochastic volatility, and stochastic local volatility models. The presented framework is part of an exciting recent stream of literature on numerical option pricing, and offers a new perspective that combines the theory of diffusion processes, Markov chains, and Fourier techniques. It is also elegantly connected to partial differential equation (PDE) approaches.

1 Introduction

Markov processes are ubiquitous in finance, as they provide important building blocks for constructing stochastic models to describe the dynamics of financial assets. A representative Markov process that is widely used is the diffusion process, which is characterized through a stochastic differential equation (SDE). Diffusion processes evolve continuously in time and in state, and there is usually limited analytical tractability except for a few very special cases, thus an efficient and accurate approximation method is needed. In general, there are two possible directions for approximating a diffusion process:

Zhenyu Cui
School of Business, Stevens Institute of Technology, Hoboken, NJ 07030. e-mail: zcui6@stevens.edu

J. Lars Kirkby
School of Industrial and Systems Engineering, Georgia Institute of Technology, Atlanta, GA 30318 e-mail: jkirkby3@gatech.edu

Duy Nguyen
Corresponding Author. Department of Mathematics, Marist College, Poughkeepsie, NY 12601 e-mail: nducduy@gmail.com

G. Yin and Q. Zhang (eds.), *Modeling, Stochastic Control, Optimization, and Applications*, The IMA Volumes in Mathematics and its Applications 164,
https://doi.org/10.1007/978-3-030-25498-8_6

1. *Time discretization*: discretize the time space into a finite discrete grid of time points, while preserving the continuous state space of the diffusion process, and then approximate the evolution of the diffusion process through time-stepping. Representative methods in this category include the Euler discretization as well as higher order time-stepping schemes (see [36] for a comprehensive account of existing methods), and the Ito-Taylor expansion method which is based on iterative applications of the Dynkin formula and fundamental properties of infinitestimal generators of the diffusion process.
2. *State discretization*: discretize the state space into a finite discrete grid of spatial points, while preserving the continuous time dimension of the diffusion process, and then approximate the evolution of the diffusion process through a continuous-time Markov chain (CTMC). A CTMC is a natural approximation tool here as it evolves continuously in time, and its transition density can be completely characterized through the *rate matrix* or *generator matrix*, which is a (discrete-state) analogue to the infinitestimal generator of the diffusion process.

There are pros and cons associated with either of the above two possible approximation methods, which will be discussed in details in subsequent sections. The previous (finance and economics) literature has mainly focused on the first approach, which we briefly summarize below:

- The Euler discretization has been very popular in numerical solutions of SDEs arising in finance, e.g. the Cox-Ingersoll-Ross (CIR) process. The convergence properties of the discretization scheme, and careful handling of the boundary behaviors have been discussed in the literature, see [35]. The Euler method is also the pillar for the "simulated maximum likelihood estimation" (SMLE) popular in financial econometrics, see [22]
- The Ito-Taylor expansion is based on a small-time expansion, and it has been applied in parameter estimation of diffusion process (see [3]), and options pricing (see [46]).

On the other hand, the second approximation approach has a relatively thinner literature and has received much less attention from academics in finance and economics. Thus it is our focus to survey the recent literature on CTMC approximation methods applied to options pricing. A brief summary of the extant literature is as follows:

- The Markov chain approximation method was first developed in the setting of general stochastic control theory, for which it yields tractable solutions for general Markovian control problems, see [44]. Note, however, that the main tool employed there is the discrete-time Markov chain (DTMC). The more specific application to finance (e.g. the Merton optimal investment and consumption problem) has been considered in [55].
- In the realm of options pricing, to the best of authors' knowledge, the DTMC method was first applied in the GARCH option pricing setting, see [19, 20].

- The above previous literature concerns the DTMC method, and some of the more recent literature considers applying the CTMC method to both path-independent and path-dependent options pricing, see some of the recent developments in [8, 14, 54, 71, 72, 73]. Rigorous convergence analysis for the CTMC approximation method has been established in [47, 70] for the case of path-independent options, and in [53, 61] for the case of a class of path-dependent options (e.g. arithmetic Asian option and step option, which is based on the occupation time.).

Regime switching models are popular in financial applications, such as time series modeling (see [29]), interest rate/foreign exchange rate movements (see [4]), credit rating transitions (see [6]), economic booms and recessions (see [39]), stock trading (see [74]) etc. It has also been popular in the options pricing and portfolio choice literature, see for example [75, 76]. Note that most of the previous literature mentioned above concerns the regime switching model itself. Regime switching models are closely related to the continuous-time Markov chain. Intuitively, we can think of a CTMC as a stochastic process making transitions among a finite number of "regimes". Regime switching models also reflect the idea of "random volatility", since we can understand the different regime levels as corresponding to different volatility levels for the financial asset of interest. Motivated by these two insights, there is recent development in the literature utilizing the regime switching model as an approximation tool for continuous stochastic volatility models. The method reduces a multi-factor stochastic volatility model to a one-dimensional diffusion model subject to regime switching, and handy analytical expressions have been developed, see [12, 13, 14, 15, 43].

There are two major components in this chapter: first we shall describe the main ideas behind utilizing a CTMC in approximating a diffusion process, and then discuss the applications and survey the recent relevant literature; second, we depict the main ideas on regime switching approximation to continuous stochastic volatility and stochastic local volatility models.

The chapter is organized as follows: Section 2 recalls the basic theory underlying the use of a continuous time Markov chain to approximate a general diffusion process, and then presents the main method for approximating time-changed Markov processes. Section 3 presents the method for approximating general stochastic volatility models by a Markov modulated diffusion process, and furthermore by a Markov modulated CTMC for the case of stochastic local volatility models. Section 4 concludes the chapter.

2 Univariate Markov Chain Approximations

Early research in Markov chain based option pricing [9] dealt with approximating the univariate diffusion dynamics for an underlying risky asset. Our treatment starts with this case, and builds gradually to more complex dynamics, including general continuous stochastic local volatility models.

2.1 Markov Processes, Diffusion Models, and Option Pricing

Assume that we are equipped with a complete filtered probability space $(\Omega, \mathscr{F}, \mathbf{F}, \mathbb{P})$, where $\mathbf{F} = \{\mathscr{F}_t\}_{t\geq 0}$ denotes the standard filtration, and here $\mathbb{P}$ is the risk-neutral measure under which we price options. Consider a real-valued (time-homogeneous) diffusion process $\{S_t\}_{t\geq 0}$, which satisfies the following stochastic differential equation:

$$dS_t = \mu(S_t)dt + \sigma(S_t)dW_t, \quad 0 \leq t \leq T, \tag{1}$$

where W_t is a standard Brownian motion, and $\mu, \sigma : \mathbb{R} \to \mathbb{R}$ are respectively drift and diffusion functions satisfying appropriate regularity conditions so that (1) has a unique solution[1]. The random process $S = \{S_t\}_{t\geq 0}$ belongs to Markov process class, and is often used to model the price evolution of a risky asset, for example the stock price or the commodity price. For a rigorous and more in depth treatment of Markov processes, the reader is invited to refer to the monograph [24]. The diffusion characterized by (1) nests some important models in finance as special cases, such as the geometric Brownian motion (Black-Scholes model), the Cox-Ingersoll-Ross (CIR) process, etc. Assume that the state space for S is given by $\mathscr{S} = [0, \infty)$, and this is intuitive because most financial assets are positive valued. In general, we are interested in computing the following quantity:

$$\mathbb{E}[H(S_T)|S_0], \tag{2}$$

which is a conditional expectation for some payoff function H under the risk-neutral probability measure $\mathbb{P}$. For example, when $H(s) = \max(s-K, 0) = (s-K)^+$, it represents the payoff of a European call option with expiry T, and a strike price $K > 0$. This is a representative example for path-independent payoffs. As for path-dependent derivatives, [54] consider the expectation of the following form

$$\mathbb{E}[g(S_T)\mathbf{I}_{\{\tau_A > T\}} + H(S_{\tau_A})\mathbf{I}_{\{\tau_A \leq T\}}|S_0] \tag{3}$$

with $\tau_A = \inf\{t \geq 0 : S_t \in A\}$ denoting the first time that S enters the set A, which represents knock-in or knock-out events depending on contract specifications. Assuming that A represents knock-out events, then (3) concerns an option that consists of a payment $g(S_T)$ in the case the contract has not been knocked out by time T, and a rebate $H(S_{\tau_A})$ if it has. This type of (path-dependent) payoff is commonly encountered in the options market. Other variants of barrier options include the down-and-out, up-and-out, and double knock-out options. In particular, the expectation in (2) is just a special case of (3) when $A = \emptyset$.

For some special cases in which the probability density function of S is known, it is possible to obtain exact analytical expressions for $\mathbb{E}[H(S_T)|S_0]$. However, we

[1] Depending on particular applications, it can be either a strong or weak solution. Usually Lipschitz-type conditions are required for there to exist a unique strong solution (c.f. [33]). As for a unique-in-law weak solution to exist, the Engelbert-Schimidt condition (c.f. [38]) may be imposed. Since we are mainly interested in applications to options pricing, the existence of a unique-in-law weak solution is sufficient for our discussions.

note that, in general, it is difficult to compute $\mathbb{E}[H(S_T)|S_0]$ exactly for a general diffusion model. As a result, various numerical methods are considered. Some representative methods are numerical PDE methods (through the link provided by the Feynman-Kac theorem), Monte Carlo simulation methods, Fast Fourier Transform (FFT) methods (applicable only when the characteristic function of S is known), to name just a few. In this chapter, we consider an alternative yet very general approach through the use of continuous-time Markov chain approximations, which has been recently proposed in [54, 14, 49, 15] and has received appreciable attention. Next, for a bounded Borel function H, define

$$P_t H(x) := \mathbb{E}_x[H(S_t)] := \mathbb{E}[H(S_t)|S_0 = x]. \tag{4}$$

Recall that S satisfies the Markov property:

$$\mathbb{E}[H(S_{t+r})|\mathscr{F}_t] = P_r H(S_t). \tag{5}$$

From (5), by taking the expectation on both sides, it is easy to see that the family of (pricing) operators $(P_t)_{t\geq 0}$ forms a semigroup:

$$P_{t+r}H = P_t(P_r H), \quad \forall r,t \geq 0, \quad \text{and} \quad P_0 H = H. \tag{6}$$

Let $C_0(\mathscr{S})$ denote the set of continuous functions on the state space $\mathscr{S}$ that vanish at infinity. To guarantee the existence of a *version* of S with cádlág paths satisfying the (strong) Markov process, we assume the following Feller's properties:

Assumption 1 *$S = \{S_t\}_{t\geq 0}$ is a Feller process on $\mathscr{S}$. That is, for any $H \in C_0(\mathscr{S})$, the family of operators $(P_t)_{t\geq 0}$ satisfies*

- $P_t H \in C_0(\mathscr{S})$ *for any* $t \geq 0$;
- $\lim_{t\to 0} P_t H(x) = H(x)$ *for any* $x \in \mathscr{S}$.

The family $(P_t)_{t\geq 0}$ is determined by its infinitesimal generator $\mathscr{L}$, where

$$\mathscr{L}H(x) := \lim_{t\to 0^+} \frac{P_t H(x) - H(x)}{t}, \quad \forall H \in C_0(\mathscr{S}). \tag{7}$$

For the diffusion given in (1), we have

$$\mathscr{L}H(x) = \frac{1}{2}\sigma^2(x)\frac{\partial^2 H}{\partial x^2} + \mu(x)\frac{\partial H}{\partial x}. \tag{8}$$

For example, the standard Black-Scholes-Merton (BSM) model is described by $\mu(S) = (r-q)\cdot S$ and $\sigma(S) := \sigma \cdot S$, where $r, q \in \mathbb{R}$ represent the continuous rates of interest and dividends, respectively, and by abuse of notation σ is a constant volatility rate.

2.2 Markov Chain Approximation

With the basic setup in previous section, we shall discuss the construction of approximating CTMC for a particular diffusion process. In the literature, there have been various methods in the constructions, and they mainly differ in the allocation schemes of grid points to "fill up" the state space, see [49]. In this section, we shall introduce a particular method to construct the approximating CTMC, and the issue of optimal design of grids is discussed in Section 2.3. This work considers two main directions in the CTMC approximation literature. In the first case we will approximate the underlying process S_t directly, and we shall use $\bar{n}$ to denote the number of states in the CTMC approximating the underlying asset process. In the second case we approximate a related (latent) stochastic factor, such as stochastic volatility, and will use $\bar{m}$ to denote the number of states in the approximating CTMC of that stochastic factor. We start with the first approach.

Given the diffusion characterized by (1), the goal is to construct a continuous-time Markov chain $\{S_t^{\bar{n}}\}_{t\geq 0}$ taking values in $\mathbb{S}_{\bar{n}} = \{s_1, s_2, \ldots, s_{\bar{n}}\}$- the finite state-space set, and having its dynamics "close" to those of S_t. Then, $S_t^{\bar{n}}$ will be used in approximating quantities involving the original process S_t, such as expected values of path functionals. For the Markov chain $S_t^{\bar{n}}$, its transitional dynamics are described by the *rate matrix* $\mathbf{Q} = [q_{ij}]_{\bar{n}\times\bar{n}} \in \mathbb{R}^{\bar{n}\times\bar{n}}$, whose elements q_{ij} satisfy the q-property: (i) $q_{ii} \leq 0$, $q_{ij} \geq 0$ for $i \neq j$, and (ii) $\sum_j q_{ij} = 0, \forall i = 1, 2, \ldots, \bar{n}$. In terms of q_{ij}'s, the transitional probability of the CTMC $S_t^{\bar{n}}$ is given by:

$$\mathbb{P}(S_{t+\Delta t}^{\bar{n}} = s_j | S_t^{\bar{n}} = s_i, S_{t'}^{\bar{n}}, 0 \leq t' \leq t) = \delta_{ij} + q_{ij}\Delta t + o((\Delta t)^2), \tag{9}$$

where in the above expression δ_{ij} denotes the Kronecker delta. In particular, the transitional matrix is represented in the form of a matrix exponential:

$$\mathbf{P}(\Delta t) = \exp(\mathbf{Q}\Delta t) = \sum_{k=0}^{\infty} (\mathbf{Q}\Delta t)^k/(k!), \quad \Delta t > 0. \tag{10}$$

Here the finite set $\mathbb{S}_{\bar{n}}$, which is the state space of the CTMC $\{S_t^{\bar{n}}\}_{t\geq 0}$, is carefully chosen such that the state space of S_t is sufficiently covered. Details on how to choose the grid points $s_1, s_2, \ldots, s_{\bar{n}}$ are given in Section 2.3. In addition, the construction must guarantee that $S_t^{\bar{n}}$ weakly converges to its continuous counterpart S_t under appropriate technical conditions. This is particularly helpful since it guarantees that the desired expected values of well behaved path functionals converge to the true values as the grid points are made denser in the space of S_t.

To this end, for each $i \in \{1, 2, \ldots, \bar{n}-1\}$ define $k_i := v_{i+1} - v_i$, and let $\mu^+(\mu^-)$ denote respectively the positive (negative) part of the function μ. A non-uniform finite discretization of $\mathscr{L}H(x)$ in (8) is given by:

$$\mu(s_i)\left(\frac{-k_i}{k_{i-1}(k_{i-1}+k_i)}H(s_{i-1})+\frac{k_i-k_{i-1}}{k_ik_{i-1}}H(s_i)+\frac{k_{i-1}}{k_i(k_{i-1}+k_i)}H(s_{i+1})\right)$$
$$+\frac{\sigma^2(s_i)}{2}\left(\frac{2}{k_{i-1}(k_{i-1}+k_i)}H(s_{i-1})-\frac{2}{k_{i-1}k_i}H(s_i)+\frac{2}{k_i(k_{i-1}+k_i)}H(s_{i+1})\right)$$
$$=q_{i,i-1}H(s_{i-1})+q_{i,i}H(s_i)+q_{i,i+1}H(s_{i+1})=:\mathscr{L}^nH(s). \tag{11}$$

where $q_{i,j}$'s are chosen as in [49], which is recalled here

$$q_{ij}=\begin{cases}\dfrac{\mu^-(s_i)}{k_{i-1}}+\dfrac{\sigma^2(s_i)-(k_{i-1}\mu^-(s_i)+k_i\mu^+(s_i))}{k_{i-1}(k_{i-1}+k_i)}, & \text{if } j=i-1,\\ \dfrac{\mu^+(s_i)}{k_i}+\dfrac{\sigma^2(s_i)-(k_{i-1}\mu^-(s_i)+k_i\mu^+(s_i))}{k_i(k_{i-1}+k_i)}, & \text{if } j=i+1,\\ -q_{i,i-1}-q_{i,i+1}, & \text{if } j=i,\\ 0, & \text{if } j\neq i-1,i,i+1.\end{cases} \tag{12}$$

Here $\mathbf{k}:=\{k_1,k_2,\ldots,k_{\bar{n}-1}\}$ is chosen such that

$$0<\max_{1\le i\le \bar{n}-1}\{k_i\}\le\min_{1\le i\le \bar{n}}\left\{\frac{\sigma^2(s_i)}{|\mu(s_i)|}\right\}.$$

With this choice of k_i's, $\mathbf{Q}=[q_{ij}]_{\bar{n}\times\bar{n}}$ is a tridiagonal matrix. Moreover, we have

$$\sigma^2(s_i)\ge\max_{1\le i\le \bar{n}-1}\{k_i\}\cdot|\mu(s_i)|\ge\max_{1\le i\le n-1}\{k_i\}\cdot(\mu^+(s_i)+\mu^-(s_i))$$
$$\ge k_{i-1}\mu^-(s_i)+k_i\mu^+(s_i). \tag{13}$$

As a result, the q-property is satisfied: $q_{ij}\ge 0,\forall 1\le i\neq j\le\bar{n}$, and $\sum_{j=1}^{\bar{n}}q_{ij}=0, i=1,\ldots,\bar{n}$. In addition, we have the following property regarding the diagonalizability of the generator matrix $\mathbf{Q}=[q_{ij}]_{\bar{n}\times\bar{n}}$.

Theorem 1. *(Diagonalization [15]) The tridiagonal matrix* $\mathbf{Q}$ *defined in* (12) *is diagonalizable. In addition,* $\mathbf{Q}$ *has exactly* $\bar{n}$ *simple real eigenvalues satisfying* $0\ge\lambda_1>\lambda_2>\ldots>\lambda_{\bar{n}}$. *Hence, the transitional matrix* $\mathbf{P}(t)$ *has the following decomposition:*

$$\mathbf{P}(\Delta t)=\boldsymbol{\Gamma}e^{\mathbf{D}_0\Delta t}\boldsymbol{\Gamma}^{-1}\quad\textit{with}\quad\mathbf{Q}=\boldsymbol{\Gamma}\mathbf{D}_0\boldsymbol{\Gamma}^{-1}, \tag{14}$$

where $\mathbf{D}_0:=\mathrm{diag}(\lambda_1,\lambda_2,\ldots,\lambda_{\bar{n}})$ *is a diagonal matrix of the eigenvalues of* $\mathbf{Q}$, $\boldsymbol{\Gamma}=(\gamma_{ij})_{i,j=1,\ldots,\bar{n}}$ *is a matrix whose columns are the corresponding eigenvectors, and we write* $\boldsymbol{\Gamma}^{-1}=(\tilde{\gamma}_{ij})_{i,j=1,\ldots,\bar{n}}$.

Furthermore, under some appropriate conditions, it can be shown that $S_t^{\bar{n}}$ converges weakly to S_t as $\bar{n}\to\infty$. More specifically, there is the following result.

Theorem 2. *(Weak convergence [54]) Let S be a Feller process whose infinitesimal generator* $\mathscr{L}$ *does not vanish at zero and infinity. Let* $S_t^{\bar{n}}$ *be the continuous time Markov chain with the generator given in* (11). *Assume that* $\max_{s\in\mathbb{S}_{\bar{n}}}|\mathscr{L}H(s)-$

$\mathscr{L}^{\bar{n}}H(s)| \to 0$ as $\bar{n} \to \infty$ for all functions H in the core of $\mathscr{L}$ and $\lim_{s\to 0^+} \mathscr{L}H(s) = 0$, then $S_t^{\bar{n}}$ converges weakly to S_t as $\bar{n} \to \infty$. That is, $\mathbb{E}[H(S_T^{\bar{n}})|S_0] \to \mathbb{E}[H(S_T)|S_0]$ for all bounded continuous functions H.

As an illustration, consider the value of an European option $e^{-rT}\mathbb{E}[H(S_T)|S_0]$ with the payoff function $H(x) = (x-K)^+$ for a call option and $H(x) = (K-x)^+$ for a put option. Assume that $S_0 = s_i \in \mathbb{S}_{\bar{n}}$, i.e., the initial value of the stock price belongs to the state space of the CTMC, for $1 \le i \le \bar{n}$ let $\boldsymbol{e}_i$ denote the column vector of size $\bar{n}$ having the value 1 on the i-th entry and 0 elsewhere; $\boldsymbol{e}_i'$ denotes the transpose of $\boldsymbol{e}_i$. We have the following two results for the applications respectively to path-independent and path-dependent options; more details can be found in [15].

Theorem 3. *(European Option) The value of a European option written on S_T can be approximated by*

$$\mathbb{E}[e^{-rT}H(S_T)|S_0 = s_i] \approx e^{-rT}\boldsymbol{e}_i'\exp(\mathbf{Q}T)\boldsymbol{H}(S_T^{\bar{n}}),$$

where $\boldsymbol{H}(S_T^{\bar{n}})$ is an $\bar{n}\times 1$ vector whose jth entry is given by $H(s_j)$.

Theorem 4. *(Bermudan Option) Let $\Delta = T/M$, where M is the number of monitoring dates, and assume that $S_0 = s_i$. The approximate value of a Bermudan option with monitoring dates $t_0 < t_1 < \ldots < t_M$ is evaluated recursively by*

$$\begin{cases} B_M = \boldsymbol{H}(S_T^{\bar{n}}), \\ B_m = \max\{e^{-r\Delta}\boldsymbol{e}_i'\exp(\mathbf{Q}\Delta)B_{m+1}, \boldsymbol{H}(S_T^{\bar{n}})\}, m = M-1, M-2, \ldots, 0. \end{cases} \tag{15}$$

2.3 Grid and Boundary Design

In this section, we shall describe the detailed construction of the grids, and hence the state space of the approximating CTMC. As previously mentioned, there are a few ways to generate the grid points, for example, a uniform grid can be constructed from two pre-chosen left and right boundary values s_1 and $s_{\bar{n}}$, and then inserting equally-spaced grid points in between. However, intuitively the uniform grid should not perform very well, and the reason is that it may not be equally likely for the stochastic process to visit each point in its state space. For example, consider the CIR process, which is mean-reverting, and by its mean-reverting property it tends to revert to its mean level either from above or below in equilibrium. Thus it is more likely for the CIR process to visit its long-term mean level rather than the two boundary points. This indicates that we shall insert more grid points around places in the state space that are more often visited, i.e., there are dense clusters of grid points in the state space, and in general this leads to a non-uniform grid.

In the following, we construct a non-uniform grid by carefully choosing the terminal values s_1 and $s_{\bar{n}}$ so that the state space of S_t is sufficiently covered and we manage to place more points around the important values (for example, around S_0). The choice of s_1 and $s_{\bar{n}}$ depends on the boundary condition of the diffusion process.

Assume that the state space of the diffusion is given by $\mathscr{S} = (e_1, e_2)$, then we usually take $s_1 = e_1$ and $s_{\bar{n}} = e_2$. For example, in the CIR model, $\mathscr{S} = [0, \infty)$, and we take $s_1 = 0$ and $s_{\bar{n}} = L$, where L is chosen sufficiently large. Note that the detailed classification of the exact properties of the two boundaries (e.g. as inaccessible, exit or regular) does not impact our choices of s_1 and $s_{\bar{n}}$. One advantage of choosing s_1 and $s_{\bar{n}}$ according to the boundaries of S_t is that we can guarantee that the approximating CTMC has the same boundary for its state space. This indicates one clear advantage of the CTMC approximation method over time-discretization methods such as the Euler time-stepping method. It is well-known in the literature (see [52]) that the Euler time-stepping may yield a boundary bias that is hard to quantify. The reason behind this is that the approximating process from the Euler time-stepping may no longer have similar boundary behaviors as the original process.

After we have fixed the left and right boundaries of the grid, what remains is to determine the spacing of the grid points. To this end, define two constants[2] $\gamma > 0$ and $\bar{s}^{\varepsilon} > 0$, then we fix $t = T/2$, and center the grid about the mean of the process S_t by: $s_1 := \max\{\bar{s}^{\varepsilon}, \bar{\mu}(t) - \gamma\bar{\sigma}(t)\}$ if the domain of S_t is positive; otherwise $s_1 := \bar{\mu}(t) - \gamma\bar{\sigma}(t)$. We next choose $s_{\bar{n}} := \bar{\mu}(t) + \gamma\bar{\sigma}(t)$, and here we have defined $\bar{\mu}(t) := \mathbb{E}[S_t|S_0]$ and $\bar{\sigma}(t)$ as the standard deviation conditional[3] on S_0. Finally, we generate $s_2, s_3, \ldots, s_{\bar{n}-1}$ using the following procedure:

$$s_i = S_0 + \bar{\alpha} \sinh\left(c_2 \frac{i}{\bar{n}} + c_1\left(1 - \frac{i}{\bar{n}}\right)\right), \quad i = 2, 3, \ldots, \bar{n}-1,$$

where

$$c_1 = \operatorname{arcsinh}\left(\frac{s_1 - S_0}{\bar{\alpha}}\right), \quad c_2 = \operatorname{arcsinh}\left(\frac{s_{\bar{n}} - S_0}{\bar{\alpha}}\right)$$

for $\bar{\alpha} < (s_{\bar{n}} - s_1)$. This transformation concentrates more grid points near the critical point S_0, where the magnitude of non-uniformity of the grid is controlled by the parameter $\bar{\alpha}$. More specifically, a smaller $\bar{\alpha}$ results in a more nonuniform grid. For numerical computations later, we choose $\bar{\alpha} = (s_{\bar{n}} - s_1)/5$. Since S_0 is not likely a member of the variance grid, we can find the bracketing index j_0 such that $s_{j_0} \leq S_0 < s_{j_0+1}$. Holding the points s_1, s_2 constant[4], we then shift the remaining points $s_j, j \geq 2$ by $S_0 - s_{j_0}$ so that $s_{j_0} = S_0$ is now a member of the adjusted grid.

For an illustration, in Figure 1 we consider the case $S \in [s_1, s_{60}] = [0, 25]$ and $S_0 = 12.5$. A non-uniform grid of size $\bar{n} = 60$ is formed using the procedure described above. Recall that the non-uniformity of the grid is controlled by the parameter $\bar{\alpha}$: the smaller the value of $\bar{\alpha}$, the more points are placed densely around S_0, which is evident from the plot of Figure 1. It is noted that non-uniform grid has been used extensitively in the literate, for example, it has been utilized in forming the PDE grid

[2] We can increase γ to make it large enough to sufficiently cover the domain of v_t. From numerical experimentation, we find that $\gamma = 4.5$ and and $\bar{s}^{\varepsilon} = 0.00001$ are sufficient for the models considered in this work.

[3] If moments of the variance process are unknown, the grids can be fixed using $s_1 = \beta_1 S_0$ and $s_{\bar{n}} = \beta_2 S_0$. For example, we can take $\beta_1 = 10^{-3}$ and $\beta_2 = 4$.

[4] This keeps an "anchor" at the boundary in the case where $S_0 \approx 0$.

(see [63]). Non-uniform grids have also been used in options pricing, for example in [42] the authors show that non-uniform grid is more favorable as compared to the uniform grid and helps to improve the rate of convergence. A 2-dimensional plot is considered in Figure 2.

Rigorous convergence and error analyses for the CTMC approximation method to option pricing, and the optimal grid design are provided respectively in [47, 70], to which we refer the reader for more details. Regarding the prices and greeks (delta and gamma) of continuously-monitored barrier options, we briefly summarize the main findings in [70]:

1. If there is no grid coinciding with the barrier level, then the convergence can only be of first order.
2. If the barrier level is part of the grid points, then the convergence is of second order for call/put type payoffs. For digital type payoffs, it is in general of first order unless the strike is exactly at the middle two grid points, in which case there is second order convergence.
3. To summarize, there are the following two conditions necessary and sufficient for achieving second order convergence for both prices and greeks:
   - A grid point falls exactly at the barrier level;
   - The strike price is exactly at the middle of two grid points.

Non-uniform grids that satisfy the two conditions in the third item above can be easily constructed. In particular, the authors of [70] propose a class of piecewise uniform grids fulfilling these two conditions that further remove convergence oscillations. Hence, Richardson extrapolation can be applied to accelerate convergence to the third order.

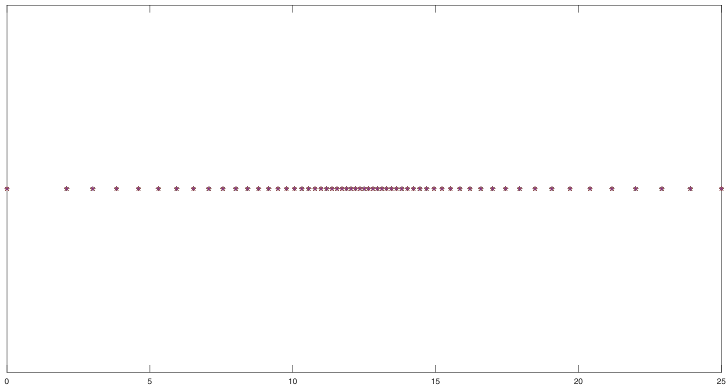

Fig. 1 Nonuniform grid plot with $S \in [0,25]$ and $\bar{n} = 60, S_0 = 12.5, \bar{\alpha} = 25/15$.

2.4 Relation to PDE

The Markov chain approximation corresponds to a state discretization, and it is of interest to see its connection to discretization methods of PDEs. In [70, 47], the connection is established between the Markov chain approximation techniques and the numerical solution to classic PDEs (see also [54]). Consider the time-homogeneous diffusion as in (1), and with natural boundaries[5] $-\infty \leq e_1 < e_2 \leq \infty$. Given a well-behaved payoff $H(\cdot)$ (for example, continuous on (e_1, e_2)), the expected value

$$u(t,x) = \mathbb{E}_x[H(S_t)]$$

satisfies the following partial differential equation (PDE)

$$\begin{aligned} &\partial_t u(t,s) = \mu(s)\partial_s u(t,y) + \frac{1}{2}\sigma^2(s)\partial_{ss}u(t,s), \quad t>0, \quad s \in (e_1,e_2), \\ &u(0,s) = H(s), \quad s \in (e_1,e_2). \end{aligned} \tag{16}$$

Recall that the continuous process S_t is approximated by the CTMC $S_t^{\bar{n}}$ with state space $\mathbb{S}_{\bar{n}} := \{s_i\}_{i=1}^{\bar{n}}$. For ease of exposition, we assume (without loss of generality) a uniform step size $k \equiv k_i = s_i - s_{i-1}$. A semi-discrete approximation is made using a central difference discretization in the space of y:

$$\begin{aligned} &\mu(s)\partial_s u(t,s) + \frac{1}{2}\sigma^2(s)\partial_{ss}u(t,s) \\ &\quad \approx \mu(s_i)\frac{u(t,s_{i+1}) - u(t,s_{i-1})}{2k} + \frac{1}{2}\sigma^2(s_i)\frac{u(t,s_{i+1}) - 2u(t,s_i) + u(t,s_{i-1})}{k^2}, \end{aligned} \tag{17}$$

with appropriate boundary conditions (e.g. reflecting, killing, or absorbing).

Let $u_k(t)$ be the approximate option price based on the discretization in (17). Then from the work of [54, 47] we have that $u_k(t)$ satisfies the following (matrix-valued) ordinary differential equation (ODE):

$$\frac{d}{dt}u_k(t) = \boldsymbol{Q}u_k(t), \qquad u_k(0) = \mathbf{H}_k, \tag{18}$$

where u_k and $\mathbf{H}_k = [H(s_1), \ldots, H(s_{\bar{n}})]^\top$ are $\mathbb{R}^{\bar{n}}$ column vectors, and $\mathbf{Q}$ is the $\bar{n} \times \bar{n}$ tridiagonal generator matrix given (12) with a constant step size k. We can solve the ODE and represent the solution as matrix exponential:

$$u_k(t) = e^{\mathbf{Q}t}\mathbf{H}_k. \tag{19}$$

Define $\pi_k g(.) = (g(y_1), g(y_2), \ldots, g(y_{\bar{n}}))^T$, and $\|A\|_\infty = \max_{i,j}|A_{i,j}|$, and consider the option written on the underlying process S_t. Let $u(\cdot)$ and $u_k(\cdot)$ denote respec-

[5] Note that we make the same assumptions (e.g. Assumption 2.1 to 2.3) as in [47], to which we refer the reader for more details.

tively the true value and the approximate option value written on S_t and $S_t^{\bar{n}}$, then we have the following result:

Theorem 5. *([47]) Suppose that H is piece-wise twice continuously differentiable (i.e., there are only a finite number of points in (e_1,e_2) where this is not true) and that at any non-differentiable point s, there exists some $\delta_s > 0$ such that H is Lipschitz continuous in $(s-\delta_s, s+\delta_s)$. Consider $k \in (0,\varepsilon)$, where ε is sufficiently small such that $\varepsilon \le \delta_s$ for all non-differentiable points s. For any $t > 0$, there is some constant $C_t > 0$ independent of k such that*

$$|| \, u_k(t) - \pi_k u(t,\cdot) \, ||_\infty \le C_t k^2. \tag{20}$$

This establishes the second order convergence from the approximate solution to the true solution.

2.5 Additive Functionals and Exotic Options

One of the benefits of the CTMC framework is the availability of closed-form pricing formulas given the relative simplicity of a finite state Markov process. Recall the transitional rate matrix $\mathbf{Q}$ and the probability transitional matrix $\mathbf{P}$ given in Section 2.2. For a function $h:\mathbb{R}\to\mathbb{R}$, define a diagonal matrix $\mathbf{D} := \mathrm{diag}(d_{jj})_{\bar{n}\times\bar{n}}$ with $d_{jj} = h(s_j)$, $j = 1,\ldots,\bar{n}$. The following Proposition 1 is concerned with the Laplace transforms of discrete and continuous additive functionals defined therein. In the following, we use M to denote number of observation points.

Proposition 1. *([14]) Define the additive functionals $B_M^{\bar{n}}$ and $A_t^{\bar{n}}$ for the CTMC $S_t^{\bar{n}}$ by:*

$$B_M^{\bar{n}} := \sum_{m=0}^{M} h(S_{t_m}^{\bar{n}}),\ k \ge 0, \quad A_t^{\bar{n}} := \int_0^t h(S_u^{\bar{n}})du,\ t \ge 0. \tag{21}$$

(i) Discrete case: $g_d(M;x) := \mathbb{E}_x\left[e^{-\theta B_M^{\bar{n}}}\right] = (e^{-\theta\mathbf{D}}\mathbf{P}(\Delta))^M e^{-\theta\mathbf{D}}\mathbf{1}$, where $\Delta := t/M$.
(ii) Continuous case: $g_c(t;x) := \mathbb{E}_x\left[e^{-\theta A_t^{\bar{n}}}\right] = e^{(\mathbf{G}-\theta\mathbf{D})t}\mathbf{1}$.

Consider the the following functions which are related to Asian options:

$$v_d(M,K,x) = \mathbb{E}_x[(B_M^{\bar{n}} - K)^+], \quad v_c(t,K,x) = \mathbb{E}_x[(A_t^{\bar{n}} - K)^+],$$

where $B_M^{\bar{n}}$ and $A_t^{\bar{n}}$ are defined in (21).

Theorem 6. *(Laplace transform of Asian option [14])*

(i) Discrete case: Let $l_d(M,\theta,x) := \int_0^\infty e^{-\theta k} v_d(M,k,x)dk$. Then for any complex number θ satisfying $Re(\theta) > 0$, we have

$$l_d(M,\theta,x) = \frac{1}{\theta^2}\left(e^{-\theta D}\exp(\mathbf{Q}\Delta)\right)^M e^{-\theta \mathbf{D}}\mathbf{1} - \frac{1}{\theta^2}\mathbf{1} + \frac{x}{\theta}\frac{1-e^{(M+1)r\Delta}}{1-e^{r\Delta}},$$

where $\mathbf{1}$ *is the* $\bar{n}\times 1$ *vector with all entries equal to* 1.

(ii) Continuous case: Let $l_c(t,\theta,x) = \int_0^\infty e^{-\theta k} v_c(t,k,x)dk$. *Then for nay complex number* θ *satisfying* $Re(\theta) > 0$, *we have*

$$l_c(t,\theta,x) = \frac{1}{\theta^2}e^{(\mathbf{Q}-\theta\mathbf{D})t}\mathbf{1} - \frac{1}{\theta^2}\mathbf{1} + \frac{x}{r\theta}(e^{rt}-1).$$

We note that the value of a discretely monitored Asian call option is given by $\frac{e^{-rT}}{M+1}v_d(M,(M+1)K,x)$, and similarly for a continuously monitored Asian call option. The results from Theorem 6 can be combined with numerical inverse Laplace transform techniques (see [1]) to price an arithmetic Asian option numerically.

Remark 1. There is a recent ground-breaking paper ([8]) that obtains the *double* transforms for the valuation of discretely-monitored and continuously-monitored arithmetic Asian options in the case when the underlying follows a CTMC. Later, [18] managed to reduce the double transforms therein to a *single* Laplace transform, which yields improved numerical performance. The topic on valuation of Asian options under different model dynamics has been of interest as reflected in recent literature, see [42, 25, 41, 10, 37, 11].

3 Regime Switching Approximations

For some applications in finance, such as volatility modeling, it is often the case that a multi-factor stochastic model is needed. One representative example is the stochastic volatility model, in which both the stock price process and the stochastic variance process (latent process that is not directly observable) are following diffusion processes. Due to the leverage effect documented in the equity market, there is usually a negative correlation between the stock price diffusion process and the variance diffusion process. It has been a challenge to decouple the non-zero correlation between the stock price and the volatility when designing approximation schemes. For example, it is a challenging task when carrying out Euler discretizations to the system of SDEs in a stochastic volatility model (see [58]).

Previous literature mostly considers the CTMC approximation of a one dimensional diffusion process, and here we shall describe a recent approach, which is developed in a series of papers ([12, 13, 14]), that has expanded the approach from univariate processes to cover multi-factor dynamics. It is based on a regime switching approximation to the stochastic volatility models, and the key insight is to simplify the dynamics in such a way that a regime switching approximation can be applied.

3.1 Markov Modulated Dynamics

Regime switching or *Markov modulated* models are a natural extension of the dynamics in (1), allowing for state dependent drift and volatility coefficients. Here the underlying (modulating) state is governed by a CTMC, $\{\alpha(t)\}_{t\geq 0}$, which takes values in $\mathscr{M} := \{1,2,\ldots,\bar{m}\}$, and is specified by its generator matrix or rate matrix, $\boldsymbol{\Lambda} = [\lambda_{ij}]_{\bar{m}\times\bar{m}}$. We denote the underlying process, which is being modulated, by $S_t^{\bar{m}}$. We model the log return process $X_t^{\bar{m}} := \log(S_t^{\bar{m}}/S_0^{\bar{m}})$, $t \in [0,T]$ by

$$dX_t^{\bar{m}} = \mu_{\alpha(t)}dt + \sigma_{\alpha(t)}dW^*(t), \tag{22}$$

where W_t^* is a standard Brownian motion independent of $\alpha(t)$, $\mu_{\alpha(t)} := r - q - \frac{1}{2}\sigma_{\alpha(t)}^2$. In particular, regime changes coincide with changes in the state of $\alpha(t)$. Between state transitions, the asset price is governed by a standard diffusion process with constant drift and volatility coefficients. This corresponds to the following model for the underlying:

$$dS_t^{\bar{m}} = S_t^{\bar{m}}(r-q)dt + S_t^{\bar{m}}\sigma_{\alpha(t)}dW^*(t). \tag{23}$$

An important property of regime-switching models is that the characteristic function (ChF) of the log-return process is available in closed-form. In particular, define the set of functions

$$\psi_j(\xi) = i\xi\mu_j - \frac{1}{2}\xi^2\sigma_j^2, \quad j = 1,\ldots,\bar{m}, \tag{24}$$

which represents the characteristic exponents of $X_t^{\bar{m}}$ when each of the states is fixed.

Lemma 1. *([7]) For $t > 0$, the characteristic function of $X_t^{\bar{m}}$ is given by the following matrix form*

$$\mathbb{E}[\exp(iX_t^{\bar{m}}\xi)|\alpha(0) = j_0] = \boldsymbol{e}'_{j_0}\exp\left(t\left(\boldsymbol{\Lambda} + diag(\psi_1(\xi),\ldots,\psi_{\bar{m}}(\xi))\right)\right)\mathbf{1}, \tag{25}$$

where $\mathbf{1} \in \mathbb{R}^{\bar{m}}$ is a unit (column) vector, and $\boldsymbol{e}_{j_0} \in \mathbb{R}^{\bar{m}}$ is a vector of zeros, except for the value 1 in the position $\alpha(0) = j_0$.

Our treatment of regime-switching models has been necessarily brief. There are several excellent further references including the following: [34, 50, 51, 56, 57, 65, 69]. For a comprehensive treatment of regime switching models, and in particular regime switching diffusion processes and their applications, please refer to monographs [66, 67, 68].

3.2 Stochastic Volatility

Consider the stochastic volatility model whose dynamics are of the following form:

$$\begin{cases} \frac{dS_t}{S_t} = \gamma(v_t)dt + \varkappa(v_t)dW_t^{(1)}, \\ dv_t = \mu_v(v_t)dt + \sigma_v(v_t)dW_t^{(2)}, \end{cases} \tag{26}$$

where $\mathbb{E}[dW_t^{(1)}dW_t^{(2)}] = \rho dt$ with $\rho \in (-1,1)$ denoting the correlation level between asset and volatility. For the model considered in (26), we assume that there exists a constant $C > 0$ such that for all v_1, v_2 in the state space of v_t

$$|\mu_v(v_1) - \mu_v(v_2)| + |\sigma_v(v_1) - \sigma_v(v_2)| \le C|v_1 - v_2|, \quad (\mu_v(v_1))^2 + (\sigma_v(v_1))^2 \le C(1 + v_1^2).$$

The above conditions guarantee that there exists a unique solution v_t possessing the strong Markov property (see [26]). Moreover, we assume that $\sigma_v(.)$ and $\varkappa(.)$ are continuously differentiable, with $\sigma_v(\cdot) > 0$ on the domain of v_t.

We sometimes call this model the "linear" stochastic volatility model since the stock price dynamic is linear in the stock price state variable S. The model (26) is very general, and encompasses many well-known SV models in the literature. A representative list of common SV models can be found in Table 1.

Heston ([31])	$dS_t = rS_tdt + \sqrt{V_t}S_tdW_t^{(1)}$ $dV_t = \eta(\theta - V_t)dt + \alpha\sqrt{V_t}dW_t^{(2)}$	$r \in \mathbb{R}$ $\eta, \theta, \alpha, v_0 > 0$
3/2 ([45])	$dS_t = rS_tdt + \sqrt{V_t}S_tdW_t^{(1)}$ $dV_t = V_t[\eta(\theta - V_t)dt + \alpha\sqrt{V_t}dW_t^{(2)}]$	$r \in \mathbb{R}$ $\eta, \theta, \alpha, v_0 > 0$
4/2 ([27])	$dS_t = rS_tdt + S_t[a\sqrt{V_t} + b/\sqrt{V_t}]dW_t^{(1)}$ $dV_t = \eta(\theta - V_t)dt + \alpha\sqrt{V_t}dW_t^{(2)}$	$r \in \mathbb{R}$ $a, b, \eta, \theta, \alpha, v_0 > 0$
Hull-White ([32])	$dS_t = rS_tdt + \sqrt{V_t}S_tdW_t^{(1)}$ $dV_t = \alpha V_tdt + \beta V_tdW_t^{(2)}$	$r \in \mathbb{R}$ $\beta, v_0 > 0$
Stein-Stein ([62])	$dS_t = rS_tdt + V_tS_tdW_t^{(1)}$ $dV_t = \eta(\theta - V_t)dt + \beta V_tdW_t^{(2)}$	$r \in \mathbb{R}$ $\beta, v_0 > 0$
α-Hypergeometric ([23])	$dS_t = rS_tdt + e^{V_t}S_tdW_t^{(1)}$ $dV_t = (\eta - \theta e^{\alpha V_t})dt + \beta V_tdW_t^{(2)}$	$r \in \mathbb{R}$ $\beta, v_0 > 0$
Jacobi ([2])	$dS_t = (r - V_t/2)dt + \sqrt{V_t - \rho^2 Q(V_t)}dW_t^{(1)}$ $dV_t = (\eta - \theta e^{\alpha V_t})dt + \beta\sqrt{Q(V_t)}dW_t^{(2)}$	$r \in \mathbb{R}$ $\beta, v_0 > 0$

Table 1 Some stochastic volatility models. For Jacobi model, we have $Q(v) := (v - v_{\min})(v_{\max} - v)/(\sqrt{v_{\max}} - \sqrt{v_{\min}})^2$.

In the next subsection, we seek to single out the correlation ρ and decouple the SDE system in (26).

3.2.1 Decoupled Dynamics

Options pricing in a general stochastic volatility model is notoriously difficult due to the general correlation structure between the two driving Brownian motions $W_t^{(1)}$ and $W_t^{(2)}$. In this section, we will provide a general procedure to decouple the correlation between the two Brownian motions. From the Ito's lemma, we have

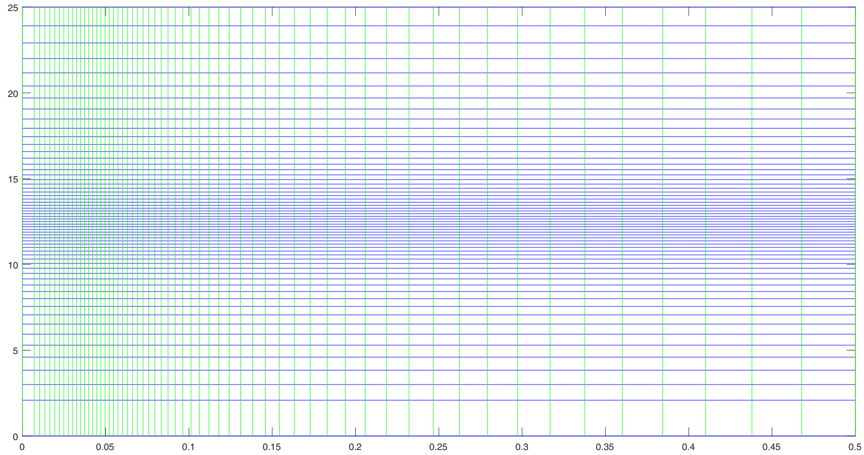

Fig. 2 Nonuniform grid plot with $(S,v) \in [0,25] \times [0,0.5]$, $\bar{n} = 60, \bar{m} = 60, S_0 = 12.5, v_0 = 0.05, \bar{\alpha}_S = 25/15, \bar{\alpha}_v = 0.5/15$.

$$d\log(S_t) = \left(\gamma(v_t) - \frac{1}{2}\varkappa^2(v_t)\right)dt + \varkappa(v_t)dW_t^{(1)}. \tag{27}$$

Next, define $\hat{f}(x) := \int_c^x \frac{\varkappa(u)}{\sigma_v(u)}du$ with c being a constant, and

$$h(x) := \mathscr{L}(\hat{f}(x)) = \mu_v(x)\hat{f}'(x) + \frac{1}{2}\sigma_v^2(x)\hat{f}''(x).$$

Denote $f(v_t, v_0) := \rho(\hat{f}(v_t) - \hat{f}(v_0))$, then we have

$$df(v_t, v_0) = \rho d\hat{f}(v_t) = \rho h(v_t)dt + \rho\varkappa(v_t)dW_t^{(2)}. \tag{28}$$

Finally, define $W_t^* := \frac{W_t^{(1)} - \rho W_t^{(2)}}{\sqrt{1-\rho^2}}$, then one can easily verify that W_t^* is a standard Brownian motion and $\mathbb{E}[dW_t^* dW_t^{(2)}] = 0$, i.e., the two Brownian motions W_t^* and $W_t^{(2)}$ are independent. Next, we plug (28) into (27), and obtain

$$\begin{aligned} d\log(S_t) &= \left(\gamma(v_t) - \frac{1}{2}\varkappa^2(v_t)\right)dt + \varkappa(v_t)(\rho dW_t^{(2)} + \sqrt{1-\rho^2}dW_t^*) \\ &= \left(\gamma(v_t) - \frac{1}{2}\varkappa^2(v_t)\right)dt + df(v_t, v_0) - \rho h(v_t)dt + \sqrt{1-\rho^2}\varkappa(v_t)dW_t^*. \end{aligned}$$

Denote $\widetilde{X}_t := \log(S_t/S_0) - f(v_t, v_0)$, then we can rewrite (26) as

$$\begin{cases} d\widetilde{X}_t = \left(\gamma(v_t) - \frac{1}{2}\varkappa^2(v_t) - \rho h(v_t)\right) dt + \sqrt{1-\rho^2}\varkappa(v_t)dW_t^*, \\ dv_t = \mu_v(v_t)dt + \sigma_v(v_t)dW_t^{(2)}. \end{cases} \tag{29}$$

Observe that the two Brownian motions in (29) are independent, and we have successfully decoupled the correlation structure. We will refer to the process $\widetilde{X}_t$ which provides the decoupling as the *auxiliary process*.[6]

3.2.2 Regime Switching Approximation: Affine Case

Using the continuous time Markov chain approximation in Section 2, we will convert (29) into a regime switching model. More specifically, for $\bar{m} \in \mathbb{N}^+$ we will approximate the variance process v_t by another independent finite state Markov chain α_t taking values in the state space $\mathscr{M} := \{1, 2, \ldots, \bar{m}\}$ with the generator $\boldsymbol{\Lambda} = [\lambda_{ij}]_{\bar{m}\times\bar{m}}$ obtained as in (12) using the dynamics of v_t given in (29). Then the model in (29) is reduced to

$$\begin{aligned} d\widetilde{X}_t^{\bar{m}} &= \left(\gamma(v_{\alpha_t})) - \frac{1}{2}\varkappa^2(v_{\alpha_t}) - \rho h(v_{\alpha_t})\right) dt + \sqrt{1-\rho^2}\varkappa(v_{\alpha_t})dW_t^*, \\ &=: \mu_X(v_{\alpha_t})dt + \sigma_X(v_{\alpha_t})dW_t^*, \end{aligned} \tag{30}$$

and note that notation-wise $v_t^{\bar{m}} = v_{\alpha_t}$, where v_{α_t} takes values in $\mathbb{S}_v := \{v_1, \ldots, v_{\bar{m}}\}$. In particular, the diffusion coefficients depend only on v_{α_t}. As with the regime-switching models discussed in Section 3.1, once $\boldsymbol{\Lambda}$ is determined, $\widetilde{X}_t^{\bar{m}}$ can be described by its generator in each state, or equivalently by its set of characteristic exponents

$$\widetilde{\psi}_j(\xi) = i\xi\mu_X(v_j) - \frac{1}{2}\xi^2\sigma_X(v_j)^2, \quad j = 1, \ldots, \bar{m}. \tag{31}$$

From Lemma 1, the ChF of $\widetilde{X}_t^{\bar{m}}$, $\mathscr{E}(\xi) = [\mathscr{E}_{j,k}]$, is given by

$$\mathscr{E}(\xi) := \mathbb{E}[\exp(i\xi\widetilde{X}_t^{\bar{m}})|\alpha(0) = j] = \boldsymbol{e}_j' \exp\left(t\left(\boldsymbol{\Lambda} + \mathrm{diag}(\widetilde{\psi}_1(\xi), \ldots, \widetilde{\psi}_{\bar{m}}(\xi)\right)\right)\mathbf{1}.$$

Moreover, we can recover the ChF of the log-return approximation as

$$\begin{aligned} \widetilde{\mathscr{E}}_{j,k}(\xi) &:= E[\exp(i\xi \cdot \log(S_t^{\bar{m}}/S_0))|\alpha(0) = j, \alpha(t) = k] \\ &= \mathscr{E}_{j,k}(\xi) \cdot \exp(i\xi \cdot f(v_k, v_j)), \end{aligned} \tag{32}$$

which follows from the original representation $\widetilde{X}_t := \log(S_t/S_0) - f(v_t, v_0)$. The availability of a closed form ChF is a key advantage of the approximation framework, as it enables the use of highly efficient Fourier transform based approaches, which we demonstrate in Section 3.2.3 for barrier options.

[6] We note that the extension of this procedure to processes with jumps is straightforward.

3.2.3 Recursive Option Pricing under Stochastic Volatility

Provided the decoupled regime-switching dynamics in (30), Lemma 1 provides a closed-form characteristic function, which enables option pricing via Fourier techniques. As an example, consider a barrier option with terminal payoff $G(X_T) = H(S_0 \exp(X_T)) = H(S_T)$, where $X_t = \ln(S_t/S_0)$, and fix a set of monitoring dates $t_m = m\Delta$, $m = 0,\dots,M$, where $\Delta = T/M$. Let $\mathscr{C}$ denote the continuation region, and $\mathscr{C}^c$ the knock-out region for X_t, so the option expires worthless if it is observed within $\mathscr{C}^c$ at any time t_m, and pays $G(X_T)$ otherwise. For a double barrier option with knockout barriers L and U in the space of S_t, $\mathscr{C} = [l_x, u_x]$ where $l_x := \ln(L/S_0)$ and $u_x := \ln(U/S_0)$ in log space.

Barrier options can priced for the SV model defined in (26) using the Markov chain approximation, which yields

$$\log(S_t^{\bar{m}}/S_0) = \widetilde{X}_t^{\bar{m}} + f(v_t^{\bar{m}}, v_0) := X_t^{\bar{m}},$$

from which $S_t^{\bar{m}} = S_0 \exp(X_t^{\bar{m}})$. The barrier option price is calculated through the following recursive procedure, starting from the known terminal values and working backwards:

$$\begin{cases} \mathscr{V}_M(X_M^{\bar{m}}, \alpha_M) = H(X_M^{\bar{m}})\mathbb{1}_{\{X_M^{\bar{m}} \in \mathscr{C}\}} \\ \mathscr{V}_m(X_m^{\bar{m}}, \alpha_m) = e^{-r\Delta}\mathbb{E}\left[\mathscr{V}_{m+1}(X_{m+1}^{\bar{m}}, \alpha_{m+1})\mathbb{1}_{\{X_m^{\bar{m}} \in \mathscr{C}\}} | X_m^{\bar{m}}, \alpha_m\right] \quad m = M-1, ..., 0, \end{cases} \tag{33}$$

where[7] $X_m^{\bar{m}} := X_{t_m}^{\bar{m}}$ and $\alpha_m = \alpha(t_m)$. By definition, $\mathscr{V}_{m+1}(X_{m+1}^{\bar{m}}, \alpha_{m+1}) = 0$ for $X_{m+1}^{\bar{m}} \in \mathscr{C}^c = [l_x, u_x]^c$.

Next define the transition probability matrix $\mathbf{P}(\Delta)$ as in (10), with elements

$$P_{jk}^{\Delta} = \mathbb{P}[\alpha(t+\Delta) = k | \alpha(t) = j], \quad j,k = 1,\dots,\bar{m},$$

which captures transitions of the volatility state. Then with $\alpha_m = j$ and $X_m^{\bar{m}} = x \in \mathscr{C}$, we have for $m = M-1, ..., 0$,

$$\begin{aligned} \mathscr{V}_m(x, j) &= e^{-r\Delta}\mathbb{E}\left[\mathscr{V}_{m+1}(X_{m+1}^{\bar{m}}, \alpha_{m+1}) | X_m^{\bar{m}} = x, \alpha_m = j\right] \\ &= e^{-r\Delta} \sum_{k=1,..,\bar{m}} P_{j,k}^{\Delta} \mathbb{E}\left[\mathscr{V}_{m+1}(X_{m+1}^{\bar{m}}, k) | X_{m+1}^{\bar{m}} = x, \alpha_m = j, \alpha_{m+1} = k\right] \\ &= e^{-r\Delta} \sum_{k=1,..,\bar{m}} P_{j,k}^{\Delta} \int_{\mathscr{C}} \mathscr{V}_{m+1}(y, k) p_{j,k}(y|x) dy, \end{aligned}$$

where we have defined the set of transition densities for the log return process for $j,k = 1,\dots,\bar{m}$

$$p_{j,k}(y|x) = \mathbb{P}[X^{\bar{m}}(\Delta) \in y + dy | X^{\bar{m}}(0) = x, \alpha(0) = j, \alpha(\Delta) = k].$$

---

[7] A European option can be priced recursively by setting $\mathscr{C} = (-\infty, \infty)$.

As demonstrated in [43], the transition densities $p_{j,k}(y|x)$ can be approximated with high efficiency using the ChF of log returns of $X_\Delta^{\bar{m}}$, $\widetilde{\mathscr{E}}_{j,k}(\xi)$, by combing the closed form expression in (32) with the Fourier method of [40].

3.2.4 Example: 4/2 model CTMC Approximation

Many prominent examples fall within the framework of dynamics (26), including those of Heston [31], Hull-White [32], Stein-Stein [62], α-Hypergeometric [23], Jacobi [2], 3/2 [45] and the 4/2 model for which we are going to illustrate in detail. We illustrate the transform required to obtain a de-correlated representation for the 4/2 model. The reader is invited to refer to Table 1 for a list of additional models that can also be similarly considered.

The 4/2 stochastic volatility model (without jumps) was recently proposed in [27], with the important property that the instantaneous volatility can be uniformly bounded away from zero (unlike Heston's model, for example). It contains the Heston model (can be thought of as a "1/2" model) and the 3/2 model as special cases, and thus earns itself the name of a "4/2" model. Extension of the 4/2 model by adding the jump component in the underlying process can be founded in [42]. The dynamics of the 4/2 model are given by

$$\begin{cases} \frac{dS_t}{S_t} = (r - q - \lambda\kappa)dt + \left[a\sqrt{v_t} + \frac{b}{\sqrt{v_t}}\right] dW_t^{(1)}, \\ dv_t = \eta(\theta - v_t)dt + \sigma_v\sqrt{v_t}dW_t^{(2)}. \end{cases} \tag{34}$$

For this model, it is assumed that the Feller's condition $2\eta\theta > \sigma_v^2$ is satisfied, and for $a, b > 0$, the volatility component is uniformly bounded away from zero, which follows from applying Cauchy's inequality to $[a\sqrt{v_t} + \frac{b}{\sqrt{v_t}}] \geq 2\sqrt{a\sqrt{v_t}\frac{b}{\sqrt{v_t}}} = 2\sqrt{ab} > 0$ for $a, b > 0$. The change of variable, which will help us remove the correlation between the two stochastic processes $W_t^{(1)}$, $W_t^{(2)}$ in (34), is given by

$$\widetilde{X}_t = \log\left(\frac{S_t}{S_0}\right) - \frac{\rho}{\sigma_v}\big(a(v_t - v_0) + b(\log(v_t) - \log(v_0))\big). \tag{35}$$

Therefore, if we denote

$$\mu_X(v_t) = \Big(\frac{a\rho\eta}{\sigma_v} - \frac{a^2}{2}\Big)v_t + \Big(\frac{\rho b\sigma_v - b^2}{2} - \frac{b\rho\eta\theta}{\sigma_v}\Big)\frac{1}{v_t} + \frac{\rho\eta}{\sigma_v}(b - a\theta) + r - q - \lambda\kappa - ab,$$

then the dynamics in (34) can be written as

$$\begin{cases} d\widetilde{X}_t = \mu_X(v_t)dt + [a\sqrt{v_t} + \frac{b}{\sqrt{v_t}}]\sqrt{(1-\rho^2)}dW_t^*, \\ dv_t = \eta(\theta - v_t)dt + \sigma_v\sqrt{v_t}dW_t^{(2)}. \end{cases} \tag{36}$$

After approximating the variance process v_t by a $\bar{m}$-state Markov chain, and substituting it into (36), we have that the dynamics in (30) are reduced to

$$d\widetilde{X}_t^{\bar{m}} = \mu_X(v_{\alpha_t})dt + \left[a\sqrt{v_{\alpha_t}} + \frac{b}{\sqrt{v_{\alpha_t}}}\right]\sqrt{(1-\rho^2)}dW_t^*, \tag{37}$$

where v_{α_t} takes values in $\mathbb{S}_v = \{v_1 v_2, \ldots, v_{\bar{m}}\}$.

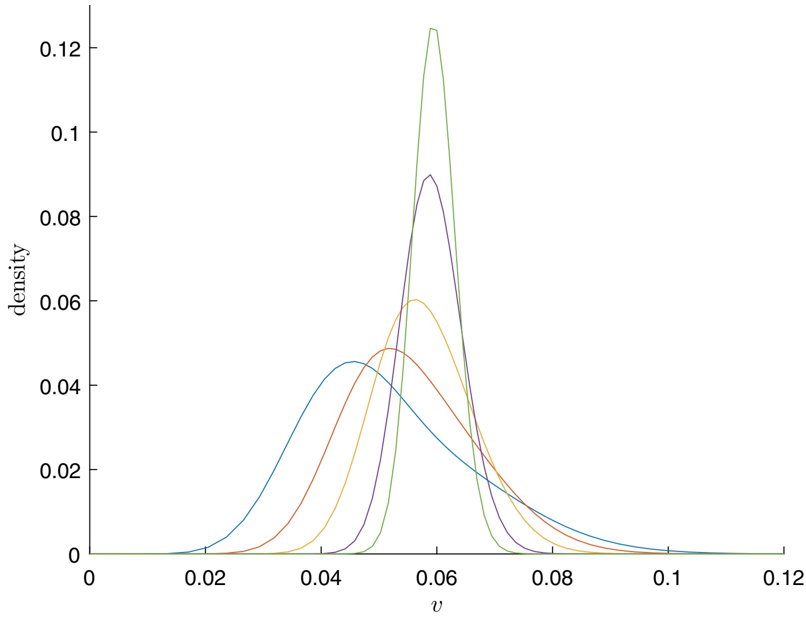

Fig. 3 Conditional transition densities of $\bar{m} = 40$ state CTMC approximation to (CIR) volatility process v_t under 4/2 (and Heston) stochastic volatility, for several values of t.

In Figure 3, we illustrate the CTMC approximation of the underlying variance process, which in the 4/2 (and Heston) model is a Cox-Ingersol-Ross (CIR) process. For $t \in \{1/5, 1/10, 1/20, 1/50, 1/100\}$, we plot the transition density of v_{α_t}, conditional on v_0, for the CIR process with $\eta = 2, \theta = 0.04, v_0 = 0.06, \rho = -0.9, \sigma_v = 0.15$. In this example, the initial variance $v_0 = 0.06$ is higher than its longer term mean, $\theta = 0.04$. When $t = 1/100$, the density is centered about v_0, and the diffusive term dominates the transition probabilities, leading to a roughly symmetric (approximately normal) transition density. As time increases up to $t = 1/5$, the densities spread out, with more mass clustering near the long term mean θ. With just $\bar{m} = 40$ points, the densities of the CTMC are a faithful representation of the underlying continuous density of v_t.

3.2.5 Example: Heston and 4/2 model option pricing

We now illustrate the application of the CTMC approximation for option pricing under the 4/2 model discussed in Section 3.2.4, starting with the special case of Heston's model, which is obtained by setting $a = 1$ and $b = 0$. The recursive pricing strategy outlined in Section 3.2.3 can be used to price European options, and in Heston's model reference prices can be obtained to machine precision using Fourier techniques (e.g. [40]). The model parameters are set to be

$$\eta = 1, \quad \theta = 0.025, \quad v_0 = 0.025, \quad \rho = -0.7, \quad \sigma_v = 0.18.$$

The state space for the CTMC approximation of v_t is determined as described in Section 2.3, with the grid width parameter $\bar{\alpha} = (v_{\bar{m}} - v_1)/\zeta$ parameterized by $\zeta > 0$. For $\zeta \approx 1$, the grid becomes uniform, while for $\zeta \approx 0$, the grid is tightly clustered around the initial variance v_0.

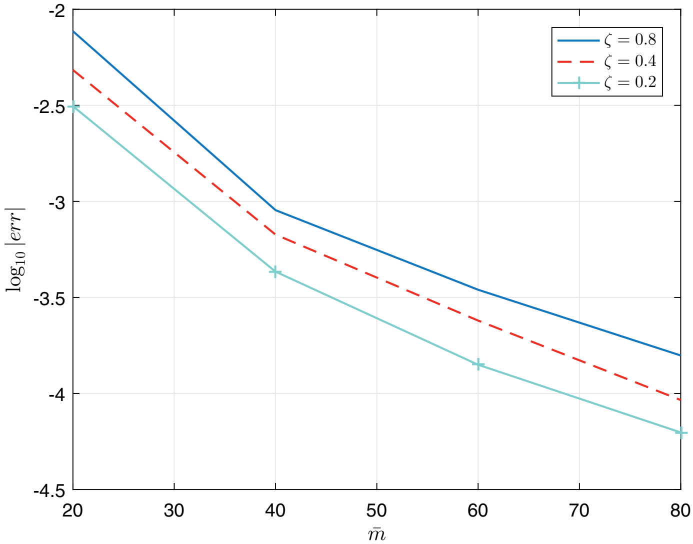

Fig. 4 European option convergence in Heston's model as a function of grid non-uniformity parameter ζ. $T = 0.5$, $K = S_0 = 100$, $r = 0.05$. Ref price: 5.7574.

Figure 4 illustrates the pricing error for an at-the-money European call option with $\zeta \in \{0.8, 0.4, 0.2\}$. As is typically the case, having a more non-uniform grid is most beneficial when the number of grid points $\bar{m}$ is small. Other factors can also influence this choice in practice, including the long term level of variance and its relation to the initial variance, as well as the time to maturity. For example, a short maturity option with initial variance near its longer term level will benefit the most from a grid which clusters around v_0, while as T increases (or equivalently σ_v increases) the benefit diminishes.

In the next set of experiments, we consider the 4/2 model, with base parameters

$$\eta = 1.8, \quad \theta = 0.04, \quad v_0 = 0.04, \quad \rho = -0.7, \quad \sigma_v = 0.1.$$

Table 2 illustrates the convergence in $\bar{m}$ for three 4/2 models, which vary based on the values of a and b. The first case, $a = 1, b = 0$, is simply Heston's model, while the other two cases have the additional variance term $b/\sqrt{v_t}$ from (36). Reference prices, to which the approximations have converged within four decimal places in the last row ($\bar{m} = 60$), are computed using $\bar{m} = 120$.

	$a = 1, b = 0$		$a = 0.5, b = 0.5v_0$		$a = 0.5, b = 0.25v_0$	
$\bar{m}$	price	error	price	error	price	error
10	6.9020	1.46e-03	6.9623	5.51e-02	5.5935	5.16e-02
20	6.8999	5.93e-04	6.9066	5.47e-04	5.5414	4.25e-04
40	6.9005	3.68e-05	6.9071	9.98e-05	5.5418	5.36e-05
60	6.9005	2.43e-06	6.9071	3.22e-05	5.5419	1.42e-05

Table 2 European call option prices under 4/2 model. $T = 0.5$, $K = S_0 = 100$, $r = 0.05$.

3.3 Regime Switching CTMCs

In Section 3.2, we discussed the use of a CTMC to approximate one dimension of the two-dimensional stochastic volatility model, which resulted in a regime-switching diffusion. Taking this idea one step further, we can consider the case of a Markov modulated CTMC, i.e., a regime switching CTMC. In this case, the $\bar{n}$-state CTMC $S_t^{\bar{n}}$ is further modulated by a second independent CTMC, $\{\alpha_t\}_{t\geq 0}$, with state space $\mathscr{M} = \{1,\dots,\bar{m}\}$. Then we have a RS-CTMC, denoted as $S_t^{\bar{n},\bar{m}}$, of the following form:

$$dS_t^{\bar{n},\bar{m}} = S_t^{\bar{n},\bar{m}}(r-q)dt + S_t^{\bar{n},\bar{m}}\sigma_{\alpha(t)}dW^*(t). \tag{38}$$

In particular, conditioned on $\alpha_t = l$, the instantaneous transitions of $S_t^{\bar{n},\bar{m}}$ can be described by the following generator $\mathscr{G}_l$, $l \in \mathscr{M}$:

$$\mathscr{G}_l h(x) := \lim_{\delta\downarrow 0} \frac{\mathbb{E}\left[h(S_{t+\delta}^{\bar{n},\bar{m}})|\alpha(t) = l, S_t^{\bar{n},\bar{m}} = x\right] - h(x)}{\delta}, \tag{39}$$

which corresponds to a rate matrix $\mathbf{G}_l = (g_{kj}^l)_{\bar{n}\times\bar{n}}$. An explicit example of $\mathbf{G}_l$ will be given in Section 3.4.2.

In Section 3.4, we consider the applications of regime switching Markov chain approximation to several options pricing problems. In the following, we shall discuss the details of the regime switching approximation in two types of models in increasing order of generality: the stochastic volatility(SV) model, and the stochastic local volatility(SLV) model. In the SV model, we utilize one approximating CTMC, and for the case of the SLV model, there are two independent approximating CTMCs introduced.

3.4 Stochastic Local Volatility

The proposed valuation framework is also applicable to general stochastic local volatility models whose dynamics are given by:

$$\begin{cases} dS_t = \omega(S_t, v_t)dt + \varkappa(v_t)\Gamma(S_t)dW_t^{(1)}, \\ dv_t = \mu_v(v_t)dt + \sigma_v(v_t)dW_t^{(2)}, \end{cases} \tag{40}$$

where $\mathbb{E}[dW_t^{(1)}dW_t^{(2)}] = \rho dt$ with $\rho \in (-1,1)$. Here we assume that $\omega(\cdot,\cdot) : \mathbb{R} \times \mathbb{R} \to \mathbb{R}$, $\varkappa(\cdot) : \mathbb{R} \to \mathbb{R}_+$ and $\Gamma(\cdot) : \mathbb{R} \to \mathbb{R}_+$. Some representative local volatility models are listed in Table 3. We make the following assumption about the Feller property of (S_t, v_t).

Assumption 2 *For any $\Phi \in C_0(\mathbb{S} \times \mathbb{V})$, define the pricing operator $P_t\Phi(S,v) := \mathbb{E}[\Phi(S_t, v_t)|S_0 = S, v_0 = v]$, and assume that (S_t, v_t) is a Feller process, i.e.,*

- $P_t\Phi \in C_0(\mathbb{S} \times \mathbb{V})$ *for any* $t \geq 0$;
- $\lim_{t\to 0} P_t\Phi(S,v) = \Phi(S,v)$ *for any* $(S,v) \in \mathbb{S} \times \mathbb{V}$.

The Feller property guarantees that there exists a *version* of the process (S_t, v_t) with cádlág paths satisfying the strong Markov property. Similar to the scalar case, the family (P_t) is determined by its infinitesimal generator $\mathscr{L}^S$, where

$$\mathscr{L}^S\Phi(S,v) := \lim_{t\to 0^+} \frac{(P_t\Phi - \Phi)(S,v)}{t}, \tag{41}$$

for any $\Phi \in C_0(\mathbb{S} \times \mathbb{V})$ for which the right-hand side of (41) converges in the strong sense.[8] From (40), we can calculate

$$\mathscr{L}^S\Phi = \frac{[\varkappa(v)\Gamma(S)]^2}{2}\frac{\partial^2\Phi}{\partial S^2} + \rho\varkappa(v)\Gamma(S)\sigma(v)\frac{\partial^2\Phi}{\partial v\partial S} + \\ + \frac{\sigma_v^2(v)}{2}\frac{\partial^2\Phi}{\partial v^2} + \omega(S,v)\frac{\partial\Phi}{\partial S} + \mu_v(v)\frac{\partial\Phi}{\partial v}. \tag{42}$$

For example, for the classical SABR model, see Table 3, the generator is given by

[8] Convergence is with respect to the norm $\|\Phi\| := \sup_{(s,v)\in\mathbb{S}\times\mathbb{V}} |\Phi(s,v)|$ on the Banach space $(C_0(\mathbb{S}\times\mathbb{V}), \|\cdot\|)$. The domain of $\mathscr{L}^S$ is dense in $C_0(\mathbb{S}\times\mathbb{V})$.

$$\mathscr{L}^S\Phi = \frac{1}{2}v^2S^{2\beta}\frac{\partial^2\Phi}{\partial S^2} + \rho\alpha v^2S^\beta\frac{\partial^2\Phi}{\partial v\partial S} + \frac{1}{2}(\alpha v)^2\frac{\partial^2\Phi}{\partial v^2}.$$

3.4.1 Decoupled Dynamics

Define the functions $g(x) := \int_\cdot^x \frac{1}{\Gamma(u)}du$ and $\hat{f}(x) := \int_\cdot^x \frac{\varkappa(u)}{\sigma_v(u)}du$, and let $\widetilde{X}_t := g(S_t) - \rho\hat{f}(v_t)$. Then similarly to the stochastic volatility case, the dynamics in (40) can be rewritten as

$$\begin{cases} d\widetilde{X}_t = \left(\frac{\omega(S_t,v_t)}{\Gamma(S_t)} - \frac{\Gamma'(S_t)}{2}\varkappa^2(v_t) - \rho h(v_t)\right)dt + \sqrt{1-\rho^2}\varkappa(v_t)dW_t^*, \\ dv_t = \mu_v(v_t)dt + \sigma_v(v_t)dW_t^{(2)}, \end{cases} \tag{43}$$

where

$$\begin{aligned} h(x) &:= \mathscr{L}^v f(x) = \mu_v(x)\hat{f}'(x) + \frac{1}{2}\sigma_v^2(x)\hat{f}''(x) \\ &= \mu_v(x)\frac{\varkappa(x)}{\sigma_v(x)} + \frac{1}{2}\left(\sigma_v(x)\varkappa'(x) - \sigma_v'(x)\varkappa(x)\right). \end{aligned} \tag{44}$$

We shall carry out the approximation procedure in *two layers*: one for the stochastic variance process, and one for the asset price process. The first layer approximation is obtained by replacing v_t with $v_t^{\bar{m}} = v_{\alpha(t)}$, and we obtain

$$\widetilde{X}_t^{\bar{m}} := g(S_t^{\bar{m}}) - \rho\hat{f}(v_t^{\bar{m}}),$$

where $S_t^{\bar{m}}$ is used to denote the dependence of S_t on $v_t^{\bar{m}}$. Next, let

$$\zeta_0(\widetilde{X}_t^{\bar{m}}, v_t^{\bar{m}}) := g^{-1}(\widetilde{X}_t^{\bar{m}} + \rho f(v_t^{\bar{m}})),$$

and for any fixed state $v_l \in \mathbb{S}_v$, define

$$\tilde{\omega}(\cdot, v_l) := \omega(\zeta_0(\cdot, v_l), v_l), \quad \tilde{\Gamma}(\cdot, v_l) := \Gamma(\zeta_0(\cdot, v_l)).$$

We further define:

$$\mu_X(x, v_l) := \left(\frac{\tilde{\omega}(x,v_l)}{\tilde{\Gamma}(x,v_l)} - \frac{\tilde{\Gamma}'(x,v_l)}{2}\varkappa^2(v_l) - \rho h(v_l)\right), \tag{45}$$

where $\tilde{\Gamma}'(\cdot, v_l) = \Gamma'(\zeta_0(\cdot, v_l))$. We manage to obtain the following dynamics for $\widetilde{X}_t^{\bar{m}}$ conditional on the value of $v_t^{\bar{m}}$:

$$d\widetilde{X}_t^{\bar{m}} = \mu_X(\widetilde{X}_t^{\bar{m}}, v_t^{\bar{m}})dt + \sqrt{1-\rho^2}\varkappa(v_t^{\bar{m}})dW_t^*. \tag{46}$$

3.4.2 Regime Switching Approximation: Linear and Nonlinear Case

The insight of [14] is to combine the RS-CTMC representation provided in Proposition 2 with a Markov chain approximation for the decoupled dynamics of the SLV model in (40). From the single layer approximation in (46), for each variance state $l \in \mathscr{M}$, the generator satisfies

$$\mathscr{L}_l^{\bar{m}}\xi(x) = \mu_X(x,v_l)\xi'(x) + \frac{(1-\rho^2)\varkappa^2(v_l)}{2}\xi''(x). \tag{47}$$

We then make a second layer approximation, similarly as before. In particular, for each $l \in \mathscr{M}$, the rate matrix is given by $\mathbf{G}_l = (g_{kj}^l)$, where

$$g_{kj}^l = \begin{cases} \dfrac{\mu_X{}^-(x_k,v_l)}{\delta_{k-1}^x} + \dfrac{\tilde{\sigma}^2(v_l) - [\delta_{k-1}^x\mu_X{}^-(x_k,v_l) + \delta_k^x\mu_X{}^+(x_k,v_l)]}{\delta_{k-1}^x(\delta_{k-1}^x+\delta_k^x)}, & j=k-1, \\ \dfrac{\mu_X{}^+(x_k,v_l)}{\delta_k^x} + \dfrac{\tilde{\sigma}^2(v_l) - [\delta_{k-1}^x\mu_X{}^-(x_k,v_l) + \delta_k^x\mu_X{}^+(x_k,v_l)]}{\delta_k^x(\delta_{k-1}^x+\delta_k^x)}, & j=k+1, \\ -q_{k,k-1}^l - q_{k,k+1}^l, & j=k, \\ 0, & |j-k|>1, \end{cases} \tag{48}$$

where $\tilde{\sigma}(v_l) = \sqrt{1-\rho^2}\varkappa(v_l)$ and $\delta_k^x = x_k - x_{k-1}$ for $k = 1,2,\ldots$.

The generator is approximated for $l \in \mathscr{M}, k \in \mathscr{N}$ by

$$\mathscr{L}_l^{\bar{n},\bar{m}}\xi(x_k) = \sum_{j=1}^{\bar{n}} g_{kj}^l\xi(x_j) = \sum_{j=1}^{\bar{n}} g_{kj}^l(\xi(x_j)-\xi(x_k)). \tag{49}$$

The key insight of the paper [60] is that we can represent the RS-CTMC $S_t^{\bar{n},\bar{m}}$ as a one-dimensional process, by embedding it into a Markov chain, called Y_t, with an enlarged state space $\mathbb{S}_Y$, which is defined in the following result. The state space of the two-dimensional process $S_t^{\bar{n},\bar{m}}$ is mapped bijectively to that of Y_t, $\mathbb{S}_Y$, by the function $\phi(\cdot)$ defined below. The space $\mathbb{S}_Y$ can be interpreted as indexing $\bar{m}$ consecutive copies of $\mathbb{S}_X$, one for each of the modulating states $l \in \mathscr{M}$. Thus

Proposition 2. *([60]) Suppose that $\{S_t^{\bar{n},\bar{m}}, t \geq 0\}$ is a discrete state regime-switching CTMC, and consider another one-dimensional CTMC $\{Y_t, t \geq 0\}$ with state space $\mathbb{S}_Y := \{1,2,...,\bar{n}\cdot\bar{m}\}$ and $\bar{n}\cdot\bar{m}\times\bar{n}\cdot\bar{m}$ transition rate matrix*

$$\mathbf{G} = \begin{pmatrix} \lambda_{11}\mathbf{I}_{\bar{n}} + \mathbf{G}_1 & \lambda_{12}\mathbf{I}_{\bar{n}} & \cdots & \lambda_{1\bar{m}}\mathbf{I}_{\bar{n}} \\ \lambda_{21}\mathbf{I}_{\bar{n}} & \lambda_{22}\mathbf{I}_{\bar{n}} + \mathbf{G}_2 & \cdots & \lambda_{2\bar{m}}\mathbf{I}_{\bar{n}} \\ \vdots & \vdots & \ddots & \vdots \\ \lambda_{\bar{m}1}\mathbf{I}_{\bar{n}} & \lambda_{\bar{m}2}\mathbf{I}_{\bar{n}} & \cdots & \lambda_{\bar{m}\bar{m}}\mathbf{I}_{\bar{n}} + \mathbf{G}_{\bar{m}} \end{pmatrix}, \tag{50}$$

where $\mathbf{I}_{\bar{n}}$ is the $\bar{n}\times\bar{n}$ identity matrix, $\mathbf{G}_l = (g_{kj}^l)_{\bar{n}\times\bar{n}}$, and $\mathbf{\Lambda} = (\lambda_{k,j})_{\bar{m}\times\bar{m}}$. Define the mapping $\phi : \mathbb{S}_X \times \mathscr{M} \to \mathbb{S}_Y$ by $\phi(x_k,l) = (l-1)j+k$, and its inverse $\phi^{-1} : \mathbb{S}_Y \to \mathbb{S}_X \times \mathscr{M}$ by $\phi^{-1}(j) = (x_k,l)$ for $j \in \mathbb{S}_Y$, where k is the unique integer satisfying

$j=(l-1)\bar{n}+k$ for some $l\in\{1,2,\dots,\bar{m}\}$. Then we have

$$\mathbb{E}\left[\Psi(S^{\bar{n},\bar{m}},\alpha)\mid\alpha(0)=i,S_0^{\bar{n},\bar{m}}=x_k\right]=\mathbb{E}[\Psi\circ\phi^{-1}(Y)\mid Y_0=(i-1)\bar{n}+k],\quad(51)$$

for any path-dependent payoff function Ψ such that the expectation on the left hand side is finite. Here we have defined $S^{\bar{n},\bar{m}}:=(S_t^{\bar{n},\bar{m}})_{0\le t\le T}$, $\alpha:=(\alpha(t))_{0\le t\le T}$, and $Y:=(Y_t)_{0\le t\le T}$.

From this representation, [14] are able to derive closed-form pricing formulas for European, barrier, occupation time, and Asian options. Under appropriate conditions, it can be showed that $(S_t^{\bar{n},\bar{m}},v_t^{\bar{m}})$ converges weakly to (S_t,v_t) as $\bar{n},\bar{m}\to\infty$. The reader is invited to refer to [14] for more details. An extension of theoretical results and applications to time-changed Markov processes is given in [15].

3.5 European options pricing

Vanilla option prices for the underlying S_T can now be approximated with respect to

$$S_T^{\bar{n},\bar{m}}:=g^{-1}(\widetilde{X}_T^{\bar{n},\bar{m}}+\rho f(v_{\alpha_T})),\quad(52)$$

which is the discrete-space asset process corresponding to $\widetilde{X}_T^{\bar{n},\bar{m}}$:

$$\mathbb{E}\left[e^{-rT}(S_T-K)^+\,\middle|\,v_0,S_0\right]\approx\mathbb{E}\left[e^{-rT}\left(S_T^{\bar{n},\bar{m}}-K\right)^+\,\middle|\,\alpha(0)=i,\widetilde{X}_0^{\bar{n},\bar{m}}=x_k\right],$$

where we assume[9] that $v_{\alpha(0)}=v_i=v_0$ is a member of the grid for some $i\in\mathscr{M}$, and $\widetilde{X}_0^{\bar{n},\bar{m}}=x_k\in\mathscr{S}_X$. From the standard CTMC theory, an explicit representation can be obtained for a European option on $S_T^{\bar{n},\bar{m}}$, in terms of the characteristics of the one-dimensional process Y_t.

Theorem 7. *([14]) Given that $\alpha(0)=i$, $\widetilde{X}_0^{\bar{n},\bar{m}}=x_k$, for maturity T and strike $K>0$, the approximate European option price at time 0 is given by*

$$\begin{aligned}\mathbb{E}\left[e^{-rT}\left(S_T^{\bar{n},\bar{m}}-K\right)^+\,\middle|\,\alpha(0)=i,\widetilde{X}_0^{\bar{n},\bar{m}}=x_k\right]&=\mathbf{e}_{i,x_k}\cdot\exp((\mathbf{G}-r\mathbf{I})T)\cdot\mathbf{H}^{(1)}\\&=e^{-rT}\cdot\mathbf{e}_{i,x_k}\cdot\exp(\mathbf{G}T)\cdot\mathbf{H}^{(1)},\quad(53)\end{aligned}$$

where $\mathbf{e}_{i,x_k}$ is a $1\times\bar{n}\bar{m}$ vector with all entries equal to 0 except that the $(i-1)\bar{n}+k$ entry is equal to 1, and $\mathbf{H}^{(1)}$ is an $\bar{n}\bar{m}\times 1$ vector with

$$H^{(1)}_{(l-1)\bar{n}+j}=\begin{cases}\left(g^{-1}(x_j+\rho f(v_l))-K\right)^+ & \textit{for a call},\\ \left(K-g^{-1}(x_j+\rho f(v_l))\right)^+ & \textit{for a put}.\end{cases}\quad(54)$$

[9] These assumptions are without loss of generality in the sense that interpolation can be readily applied otherwise. To simplify the discussion, we assume that these points are members of the grid in what follows.

During the calibration process, prices are required for many strikes at each maturity. An advantage of the proposed methodology is that once the shared key component, the matrix exponential $\exp(\mathbf{G}T)$, is (pre)computed and cached, which dominates the computational cost, a spectrum of contracts with different strikes may be priced for essentially the same cost as a single contract.

SABR ([28])	$dS_t = v_t S_t^{\beta} dW_t^{(1)}$ $dv_t = \alpha v_t dW_t^{(2)}$	$\beta \in [0,1)$ $\alpha, v_0 > 0$
$\lambda-$SABR ([30])	$dS_t = v_t S_t^{\beta} dW_t^{(1)}$ $dv_t = \lambda(\theta - v_t)dt + \alpha v_t dW_t^{(2)}$	$\beta \in [0,1)$ $\lambda, \theta, \alpha, v_0 > 0$
Shifted SABR ([5])	$dS_t = v_t (S_t + s)^{\beta} dW_t^{(1)}$ $dv_t = \alpha v_t dW_t^{(2)}$	$\beta \in [0,1)$ $s, \alpha, v_0 > 0$
Heston-SABR ([14])	$dS_t = rS_t dt + \sqrt{v_t} S_t^{\beta} dW_t^{(1)}$ $dv_t = \eta(\theta - v_t)dt + \alpha\sqrt{v_t} dW_t^{(2)}$	$r \in \mathbb{R}, \beta \in [0,1)$ $\eta, \theta, \alpha, v_0 > 0$
Quadratic SLV ([48])	$dS_t = rS_t dt + \sqrt{v_t}(aS_t^2 + bS_t + c) dW_t^{(1)}$ $dv_t = \eta(\theta - v_t)dt + \alpha\sqrt{v_t} dW_t^{(2)}$	$r \in \mathbb{R}, \beta \in [0,1)$ $a, \eta, \theta, \alpha, v_0 > 0, 4ac > b^2$
Exponential SLV ([14])	$dS_t = rS_t dt + m(v_t)(v_L + \theta \exp(-\lambda S_t)) dW_t^{(1)}$ $dv_t = \mu(v_t)dt + \sigma(v_t) dW_t^{(2)}$	$r \in \mathbb{R}, \lambda, v_L \geq 0$ $v_L + \theta \geq 0$
Root-Quadratic SLV ([14])	$dS_t = rS_t dt + m(v_t)\sqrt{aS_t^2 + bS_t + c}\, dW_t^{(1)}$ $dv_t = \mu(v_t)dt + \sigma(v_t) dW_t^{(2)}$	$r \in \mathbb{R}$ $a > 0, c \geq 0$
Tan-Hyp SLV ([14])	$dS_t = rS_t dt + m(v_t)\tanh(\beta S_t) dW_t^{(1)}$ $dv_t = \mu(v_t)dt + \sigma(v_t) dW_t^{(2)}$	$r \in \mathbb{R}$ $\beta \geq 0$
Mean-reverting-SABR ([14])	$dS_t = \kappa(\zeta - S_t)dt + m(v_t) S_t^{\beta} dW_t^{(1)}$ $dv_t = \mu(v_t)dt + \sigma(v_t) dW_t^{(2)}$	$r \in \mathbb{R}, \beta \in [0,1)$ $\kappa, \zeta, v_0 > 0$
4/2-SABR ([14])	$dS_t = rS_t dt + S_t^{\beta}[a\sqrt{v_t} + b/\sqrt{v_t}] dW_t^{(1)}$ $dv_t = \eta(\theta - v_t)dt + \alpha\sqrt{v_t} dW_t^{(2)}$	$r \in \mathbb{R}, \beta \in [0,1)$ $a, b, \eta, \theta, \alpha, v_0 > 0$

Table 3 Some stochastic local volatility models

3.5.1 Example: SABR model

A now classic SLV example which has seen tremendous application in practice is the SABR model of [30], which is specified as

$$\begin{cases} dS_t = v_t S_t^{\beta} dW_t^{(1)}, \\ dv_t = \alpha v_t dW_t^{(2)}, \end{cases} \tag{55}$$

In particular, the variance process is governed by a geometric Brownian motion. Given the practical nature of the SABR model, several approximation frameworks have been introduced to efficiently estimate implied volatiles, such as the original approach of Hagan et. al. [28], as well as the improved approximation introduced in Antonov et. al. [5]. Traditional Monte Carlo is also widely used for this model, especially for exotic options for which no known closed-form pricing formulas exist.

Figure 5 compares the CTMC approach introduced in [14] with each of these methods, using the market standard implied volatilities of European options for illustration. We see close agreement between the method of Antonov et. al. and CTMC, while the other two methods under-perform at the wings, as is well docu-

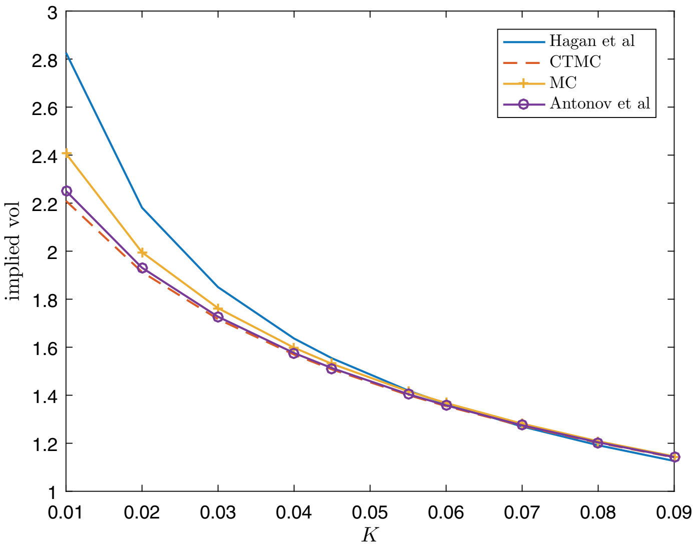

Fig. 5 SABR implied volatilities. $\alpha = 0.2, \beta = 0.1, \rho = 0, v_0 = 0.1, T = 1, S_0 = 0.05, r = 0.0$.

mented. In addition to European options, the CTMC method can be used to price American, Barrier, Asian, and occupation time derivatives in the SABR and other SLV models. Additional SLV model specifications are listed in Table 3. In particular, the $\lambda-$SABR model of [30] and the Heston-SABR model studied in [14] offer more realistic models for the variance process, as they permit mean-reversion. A further extension of the method to the shifted SABR model has been considered in [16].

4 Conclusions

This chapter reviews and consolidates recent research activity in the literature on applying continuous-time Markov chains to approximate stochastic processes arising in finance. We discuss the construction, theoretical properties and numerical performance of the CTMC approximations. We also discuss an effective regime-switching approach to approximate the dynamics of stochastic volatility models, which enables us to reduce the valuation problem to one that is concerned with a relatively simple Markov-modulated processes. In particular, explicit valuation formulas are obtained in terms of simple matrix expressions.

Since the CTMC approximation can be thought of as a state-space discretization, as compared to time-discretization schemes (e.g. the Euler scheme), a promising future research direction is to utilize this method in the efficient Monte Carlo simulation of asset prices. A first step in this direction has obtained promising results which are reported in [17]. We believe that the CTMC approximation method will find applications in various areas including the valuation, estimation and calibration of stochastic models arising in financial engineering and operations research.

References

1. Abate, Joseph, and Ward Whitt. ”The Fourier-series method for inverting transforms of probability distributions.” *Queueing Systems* 10.1-2 (1992): 5-87.
2. Ackerer, Damien, Damir Filipovic, and Sergio Pulido. “The Jacobi stochastic volatility model.” *Finance and Stochastics* (2017): 1-34.
3. Ait-Sahalia, Yacine. “Maximum likelihood estimation of discretely sampled diffusions: a closed-form approximation approach.” *Econometrica* 70, no. 1 (2002): 223-262.
4. Ang, Andrew, and Geert Bekaert. “Regime switches in interest rates.” *Journal of Business & Economic Statistics* 20, no. 2 (2002): 163-182.
5. Antonov, Alexandre, Michael Konikov, and Michael Spector. “The free boundary SABR: natural extension to negative rates.” Preprint, ssrn 2557046 (2015).
6. Bangia, Anil, Francis X. Diebold, Andr Kronimus, Christian Schagen, and Til Schuermann. “Ratings migration and the business cycle, with application to credit portfolio stress testing.” *Journal of Banking and Finance* 26, no. 2-3 (2002): 445-474.
7. Buffington, John, and Robert J. Elliott. “American options with regime switching.” *International Journal of Theoretical and Applied Finance* 5, no. 05 (2002): 497-514.
8. Cai, Ning, Yingda Song, and Steven Kou. ”A general framework for pricing Asian options under Markov processes.” *Operations Research* 63, no. 3 (2015): 540-554.
9. Chourdakis, Kyriakos, “Continuous Time Regime Switching Models and Applications in Estimating Processes with Stochastic Volatility and Jumps (November 2002)”. U of London Queen Mary Economics Working Paper No. 464. Available at SSRN: https://ssrn.com/abstract=358244 or http://dx.doi.org/10.2139/ssrn.358244
10. Chatterjee, Rupak, Zhenyu Cui, Jiacheng Fan, and Mingzhe Liu. “An efficient and stable method for short maturity Asian options.” *Journal of Futures Markets* 38 (12) (2018): 1470-1486.
11. Corsaro, Stefania, Ioannis Kyriakou, Daniele Marazzina, and Zelda Marino. “A general framework for pricing Asian options under stochastic volatility on parallel architectures.” *European Journal of Operational Research*, 272(3) (2019): 1082-1095.
12. Cui, Z, J. Lars Kirkby, and Duy Nguyen. “Equity-linked annuity pricing with cliquet-style guarantees in regime-switching and stochastic volatility models with jumps.” *Insurance: Mathematics and Economics* 74 (2017): 46-62.
13. Cui, Z, J. Lars Kirkby, and Duy Nguyen. “A general framework for discretely sampled realized variance derivatives in stochastic volatility models with jumps.” *European Journal of Operational Research* 262(1) (2017): 381-400.
14. Cui, Z, J. Lars Kirkby, and Nguyen, Duy. “A general valuation framework for SABR and stochastic local volatility models.” *SIAM Journal on Financial Mathematics* 9(2) (2018): 520-563.
15. Cui, Z., J. Lars Kirkby and Nguyen, Duy. “A general framework time-changed Markov processes and applications.” *European Journal of Operational Research*, 273(2) (2018):785-800.
16. Cui, Z., J. Lars Kirkby and Nguyen, Duy. “Full-fledged SABR through Markov Chains.” *Working paper* (2017).
17. Cui, Z., J. Lars Kirkby and Nguyen, Duy. “Efficient simulation of stochastic differential equations based on Markov Chain approximations with applications.” *Working paper* (2018).
18. Cui, Z, C. Lee, and Y. Liu. “Single-transform formulas for pricing Asian options in a general approximation framework under Markov processes.” *European Journal of Operational Research* 266, no. 3 (2018): 1134-1139.

19. Duan, Jin-Chuan, and Jean-Guy Simonato. “American option pricing under GARCH by a Markov chain approximation.” *Journal of Economic Dynamics and Control* 25, no. 11 (2001): 1689-1718.
20. Duan, Jin-Chuan, Evan Dudley, Genevive Gauthier, and J. Simonato. “Pricing discretely monitored barrier options by a Markov chain.” *Journal of Derivatives* 10 (2003).
21. Duffie, Darrell, Jun Pan, and Kenneth Singleton. “Transform analysis and asset pricing for affine jump diffusions.” *Econometrica* 68, no. 6 (2000): 1343-1376.
22. Durham, Garland B., and A. Ronald Gallant. “Numerical techniques for maximum likelihood estimation of continuous-time diffusion processes.” *Journal of Business & Economic Statistics* 20, no. 3 (2002): 297-338.
23. Da Fonseca, Jose, and Claude Martini. “The α-hypergeometric stochastic volatility model.” *Stochastic Processes and their Applications* 126.5 (2016): 1472-1502.
24. Ethier, Stewart N., and Thomas G. Kurtz. Markov processes: characterization and convergence. Vol. 282. John Wiley & Sons, (2009).
25. Fusai, Gianluca, and Ioannis Kyriakou. “General optimized lower and upper bounds for discrete and continuous arithmetic Asian options.” *Mathematics of Operations Research* 41, no. 2 (2016): 531-559.
26. Gihman, Iosif IlIch, and Anatoli Vladimirovich Skorohod. ”Stochastic differential equations.” The Theory of Stochastic Processes III. Springer, New York, NY, 1979. 113-219.
27. Grasselli, Martino. “The 4/2 stochastic volatility model: A unified approach for the Heston and the 3/2 model.” *Mathematical Finance* 27.4 (2017): 1013-1034.
28. Hagan, Patrick S., et al. ”Managing smile risk.” *The Best of Wilmott* 1 (2002): 249-296.
29. Hamilton, James D. “Analysis of time series subject to changes in regime.” *Journal of Econometrics* 45, no. 1-2 (1990): 39-70.
30. Henry-Labordere, Pierre, “A General Asymptotic Implied Volatility for Stochastic Volatility Models (April 2005)”. Available at SSRN: https://ssrn.com/abstract=698601 or http://dx.doi.org/10.2139/ssrn.698601.
31. Heston, Steven L. “A closed-form solution for options with stochastic volatility with applications to bond and currency options”. *The Review of Financial Studies 6.2 (1993): 327-343.*
32. Hull, John, and Alan White. “The pricing of options on assets with stochastic volatilities.” *The Journal of Finance* 42.2 (1987): 281-300.
33. Ikeda, Nobuyuki, and Shinzo Watanabe. “Stochastic differential equations and diffusion processes”. Vol. 24. Elsevier, (2014).
34. Jiang, Jiuxin, R. H. Liu, and D. Nguyen. “A recombining tree method for option pricing with state-dependent switching rates.” *International Journal of Theoretical and Applied Finance* 19.02 (2016): 1650012.
35. Higham, Desmond J., Xuerong Mao, and Andrew M. Stuart. “Strong convergence of Euler-type methods for nonlinear stochastic differential equations.” *SIAM Journal on Numerical Analysis* 40, no. 3 (2002): 1041-1063.
36. Jacod, Jean, and Philip Protter. “Discretization of processes”. Vol. 67. *Springer Science & Business Media*, 2011.
37. Kahale, Nabil. ”General multilevel Monte Carlo methods for pricing discretely monitored Asian options.” arXiv preprint arXiv:1805.09427 (2018).
38. Karatzas, Ioannis, and Steven Shreve. “Brownian motion and stochastic calculus”. Vol. 113. *Springer Science & Business Media*, (2012).
39. Kim, Chang-Jin, and Charles R. Nelson. “Business cycle turning points, a new coincident index, and tests of duration dependence based on a dynamic factor model with regime switching.” *Review of Economics and Statistics* 80, no. 2 (1998): 188-201.
40. Kirkby, J. Lars. “Efficient Option Pricing by Frame Duality with the Fast Fourier Transform”. *SIAM J. Financial Mathematics* Vol. 6, no.1 (2015): 713-747.
41. Kirkby, J. Lars. “An Efficient Transform Method for Asian Option Pricing”. *SIAM J. Financial Mathematics* Vol. 7, no.1 (2016): 845-892.
42. Kirkby, J. L., and D. Nguyen. “Efficient Asian option pricing under regime switching jump diffusions and stochastic volatility models”. *Working paper*, (2016).

43. Kirkby, J. Lars, Duy Nguyen, and Zhenyu Cui. “A unified approach to Bermudan and barrier options under stochastic volatility models with jumps.” *Journal of Economic Dynamics and Control* 80 (2017): 75-100.
44. Kushner, Harold, and Paul G. Dupuis. “Numerical methods for stochastic control problems in continuous time”. Vol. 24. Springer Science & Business Media, (2013).
45. Lewis, Alan L. “Option Valuation Under Stochastic Volatility II”. Finance Press, Newport Beach, CA, 2009.
46. Li, Chenxu, and Xiaocheng Li. “A closed-form expansion approach for pricing discretely monitored variance swaps.” *Operations Research Letters* 43, no. 4 (2015): 450-455.
47. Li, Lingfei, and Gongqiu Zhang. “Error analysis of finite difference and Markov chain approximations for option pricing.” *Mathematical Finance* 28.3 (2018): 877-919.
48. Lipton, A. (2002). The volatility smile problem. *Risk Magazine*. 15(2), 61-65.
49. Lo, Chia Chun, and Konstantinos Skindilias. “An improved Markov chain approximation methodology: Derivatives pricing and model calibration.” *International Journal of Theoretical and Applied Finance* 17.07 (2014): 1450047.
50. Liu, R. H. “Regime-switching recombining tree for option pricing.” *International Journal of Theoretical and Applied Finance* 13.03 (2010): 479-499.
51. Liu, R. H. ”A new tree method for pricing financial derivatives in a regime-switching mean-reverting model.” *Nonlinear Analysis: Real World Applications* 13.6 (2012): 2609-2621.
52. Lord, Roger, Remmert Koekkoek, and Dick Van Dijk. “A comparison of biased simulation schemes for stochastic volatility models.” *Quantitative Finance* 10, no. 2 (2010): 177-194.
53. Ma. J, W. Yang and Z. Cui. “Convergence rate analysis for the continuous-time Markov chain approximation of occupation time derivatives and Asian option Greeks.” *Working paper* (2018).
54. Mijatovic, Aleksandar, and Martijn Pistorius. ”Continuously monitored barrier options under Markov processes.” *Mathematical Finance* **23** (1),1–38 (2013).
55. Munk, Claus. “The Markov chain approximation approach for numerical solution of stochastic control problems: experiences from Merton’s problem.” *Applied Mathematics and Computation* 136, no. 1 (2003): 47-77.
56. Nguyen, Duy. “A hybrid Markov chain-tree valuation framework for stochastic volatility jump diffusion models.” International Journal of Financial Engineering Vol. 05, No. 04, 1850039 (2018).
57. Ramponi, Alessandro. “Fourier transform methods for regime-switching jump-diffusions and the pricing of forward starting options.” *International Journal of Theoretical and Applied Finance* 15.05 (2012): 1250037.
58. Schoebel, Rainer, and Jianwei Zhu. “Stochastic volatility with an Ornstein-Uhlenbeck process: an extension.” *Review of Finance* 3, no. 1 (1999): 23-46.
59. Scott, Louis O. “Option pricing when the variance changes randomly: Theory, estimation, and an application.” *Journal of Financial and Quantitative analysis* 22.4 (1987): 419-438.
60. Song, Yingda, Ning Cai, and Steven Kou. “A Unified Framework for Options Pricing Under Regime Switching Models.” *Working paper* (2016).
61. Song, Yingda, Ning Cai, and Steven Kou. “Computable Error Bounds of Laplace Inversion for Pricing Asian Options.” *INFORMS Journal on Computing* 30.4 (2018): 634-645..
62. Stein, Elias M., and Jeremy C. Stein. “Stock price distributions with stochastic volatility: an analytic approach.”*The review of financial studies* 4.4 (1991): 727-752.
63. Tavella, Domingo, and Curt Randall. Pricing Financial Instruments: The Finite Difference Method (Wiley Series in Financial Engineering). New York: Wiley, 2000.
64. Van der Stoep, Anthonie W., Lech A. Grzelak, and Cornelis W. Oosterlee. “The Heston stochastic-local volatility model: Efficient Monte Carlo simulation.” *International Journal of Theoretical and Applied Finance* 17.07 (2014): 1450045.
65. Yao, David D., Qing Zhang, and Xun Yu Zhou. “A regime-switching model for European options.” Stochastic processes, optimization, and control theory: applications in financial engineering, queueing networks, and manufacturing systems. Springer, Boston, MA, 2006. 281-300.

66. Yin, G. George, and Qing Zhang. Continuous-time Markov chains and applications: A two-time-scale approach. Vol. 37. Springer Science & Business Media, 2012.
67. Yin, G. George, and Qing Zhang. Discrete-time Markov chains: two-time-scale methods and applications. Vol. 55. Springer Science & Business Media, 2006.
68. Yin, George, and Chao Zhu. Hybrid switching diffusions: properties and applications. Vol. 63. New York: Springer, 2010.
69. Yuen, Fei Lung, and Hailiang Yang. "Option pricing with regime switching by trinomial tree method." *Journal of Computational and Applied Mathematics* 233.8 (2010): 1821-1833.
70. Zhang Gongqiu, and Lingfei Li. "Analysis of Markov Chain Approximation for Option Pricing and Hedging: Grid Design and Convergence Behavior." *Operations Research*. Forthcoming (2018).
71. Zhang Gongqiu, and Lingfei Li. "A general method for the valuation of drawdown risk under Markovian models." *Working paper* (2018).
72. Zhang Gongqiu, and Lingfei Li. "A unified approach for the analysis of Parisian stopping times and its applications in finance and insurance." *Working paper* (2018).
73. Zhang Gongqiu, and Lingfei Li. "A general approach for the analysis of occupation times and its applications in finance." *Working paper* (2018).
74. Zhang, Qing. "Stock trading: An optimal selling rule." *SIAM Journal on Control and Optimization* 40.1 (2001): 64-87.
75. Zhang, Qing, and Xin Guo. "Closed-form solutions for perpetual American put options with regime switching." *SIAM Journal on Applied Mathematics* 64, no. 6 (2004): 2034-2049.
76. Zhou, Xun Yu, and George Yin. "Markowitz's mean-variance portfolio selection with regime switching: A continuous-time model." *SIAM Journal on Control and Optimization* 42, no. 4 (2003): 1466-1482.